

UHASSELT



Maastricht University

KNOWLEDGE IN ACTION

Faculty of Medicine and Life Sciences
School for Life Sciences

Master of Biomedical Sciences

Master's thesis

Translocation of airborne black carbon particles from mother to unborn child: an ENVIRONAGE birth cohort study

Liesa Engelen

Thesis presented in fulfillment of the requirements for the degree of Master of Biomedical Sciences, specialization Environmental Health Sciences

SUPERVISOR :

Prof. dr. Tim NAWROT

MENTOR :

Mevrouw Eva BONGAERTS

Transnational University Limburg is a unique collaboration of two universities in two countries: the University of Hasselt and Maastricht University.



UHASSELT

KNOWLEDGE IN ACTION

www.uhasselt.be
Universiteit Hasselt
Campus Hasselt:
Martelarenlaan 42 | 3500 Hasselt
Campus Diepenbeek:
Agoralaan Gebouw D | 3590 Diepenbeek

2020
2021



Maastricht University

Faculty of Medicine and Life Sciences

School for Life Sciences

Master of Biomedical Sciences

Master's thesis

Translocation of airborne black carbon particles from mother to unborn child: an ENVIRONAGE birth cohort study

Liesa Engelen

Thesis presented in fulfillment of the requirements for the degree of Master of Biomedical Sciences, specialization Environmental Health Sciences

SUPERVISOR :

Prof. dr. Tim NAWROT

MENTOR :

Mevrouw Eva BONGAERTS

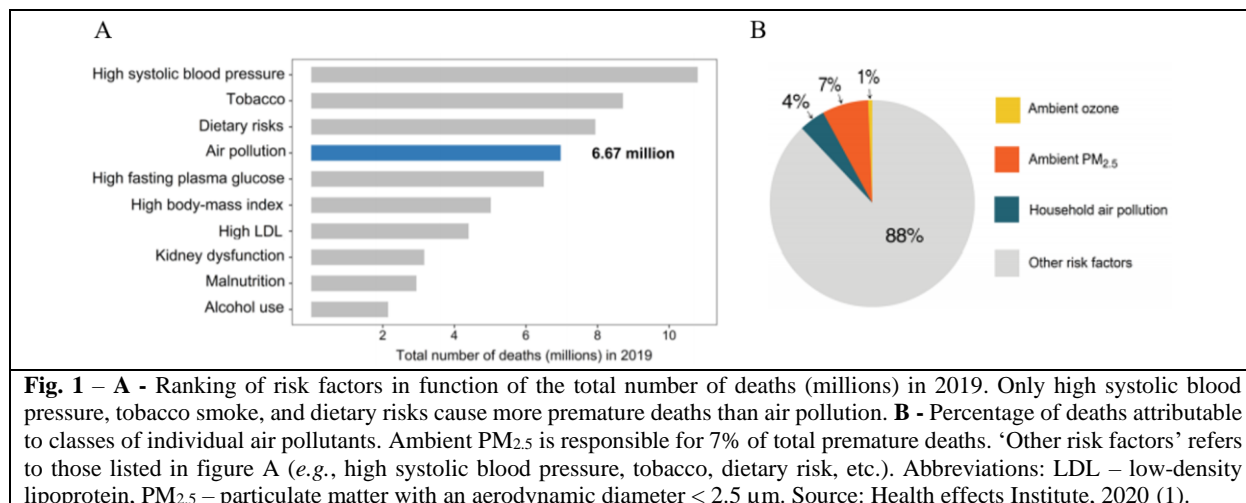
**Translocation of airborne black carbon particles from mother to unborn child:
an ENVIRONAGE birth cohort study***Liesa Engelen¹, Eva Bongaerts² and Tim S. Nawrot^{2,3}¹School of Environmental Health Sciences, Universiteit Hasselt, Campus Diepenbeek,
Agoralaan Gebouw D - 3590 Diepenbeek, Belgium²Centre for Environmental Sciences, Universiteit Hasselt, Campus Diepenbeek,
Agoralaan Gebouw D - 3590 Diepenbeek, Belgium³Department of Public Health and Primary Care, KU Leuven, Herestraat 49,
Box 703 – 3000 Leuven, Belgium*Running title: *Maternal-fetal transfer of black carbon particles*To whom correspondence should be addressed: Tim S. Nawrot, Tel: +3211268382;
Email: tim.nawrot@uhasselt.be**Keywords:** Black carbon, placental translocation, umbilical cord blood, black carbon biodistribution
femtosecond pulsed laser illumination**ABSTRACT**

The placenta was initially seen as an impenetrable barrier, protecting the fetus against toxicants. However, recent evidence demonstrated accumulation of black carbon (BC) particles in human placenta following real-life exposure. As it remains unknown whether BC particles can cross the placenta and reach the fetal circulation, we aim to detect these particles in cord blood. Cord and maternal blood samples from low (n=10) and high (n=10) exposed mother-newborn pairs enrolled in the ENVIRONAGE birth cohort were screened for the presence of BC particles. Direct and label-free detection of BC was performed using white-light generation under femtosecond pulsed laser illumination. Additionally, BC uptake in key placental cells was determined by immunofluorescence. BC particles were detected in all screened placentae and blood samples. Results revealed a higher BC load in placenta (p=0.0164), maternal (p=0.0002) and umbilical cord blood (p<0.0001) of the high exposed mothers. In addition, Pearson correlation coefficients demonstrated positive correlations between residential BC exposure during pregnancy and the measured BC load in placenta (r=0.48, p=0.034), maternal (r=0.66, p=0.002) and cord blood (r=0.90, p<0.0001). Furthermore, BC particles accumulated in all examined placental cell types; however, trophoblasts showed the highest accumulation (p=0.0038). We demonstrate that BC particles are internalized by key placental tissue cells and cross the placenta to reach the fetal circulation. These findings provide insight into real-life fetal exposure to combustion-derived particles during the most susceptible period of life, suggesting a potential link between prenatal air pollution exposure and adverse health outcomes in later life.

INTRODUCTION

In 2019, annual levels of particulate matter with an aerodynamic diameter less than 2.5 µm (PM_{2.5}), exceeded the air quality guideline of 10 µg/m³ set by the World Health Organization in more than 90% of the world's population (1). In this regard, ambient air pollution exposure is responsible for 6.67 million premature deaths worldwide each year, accounting for 12% of the

total number of deaths (Figure 1) (1). From the latter, we conclude that air pollution is the number one environmental risk factor for premature death, with only high systolic blood pressure (10.8 million), tobacco smoke (8.71 million), and dietary risks (7.94 million) bearing a superior risk (1).



Air pollution comprises a heterogeneous mixture, of which particulate matter (PM) is a key component regarding adverse health effects. PM encompasses solid matter (e.g., particles), microscopic liquid droplets, and gases. Sulfates, nitrates, ammonium, elemental and organic carbons, biological materials (e.g., bacteria, viruses), dust, metals, organic chemicals, acids, hydrocarbons, nitric oxide, and carbon monoxide, amongst others, can be defined as PM (2-4). Particles are categorized, based on their size, as ultrafine particles or PM_{0.1} (aerodynamic diameter < 0.1 μm), fine particles or PM_{2.5} (aerodynamic diameter < 2.5 μm), and coarse particles or PM₁₀ (aerodynamic diameter < 10 μm) (3, 5). This master’s thesis focuses on the most toxic component of PM_{2.5}, black carbon (BC) (6). BC is the light-absorbing component of PM_{2.5} and comprises elemental and organic carbon (7-9). These particles are the product of incomplete combustion of fossil- and biofuels, and therefore, traffic (especially diesel-driven vehicles) is a major source (9). Additionally, industrial and residential emissions, as well as open biomass burning (e.g., forest fires and agricultural waste burning), contribute to BC emissions (9, 10).

Among BC particles, there exists a lot of heterogeneity regarding physicochemical characteristics, including shape, size, mass, surface area and zeta potential (5, 11). The toxic character of BC particles is attributable to their strong surface reactivity, chemical composition and physical properties (12). Their small size results in a high surface-to-volume ratio which makes these

particles easy accessible for the adhesion of impurities, such as polycyclic aromatic hydrocarbons (PAHs), benzene, and transition metals after emission in the atmosphere (10, 13-16). In addition, the zeta potential of the particles ensures the adsorption of these particles on cell membranes, pursued by their uptake inside the cell (11). Here, they can potentially bind to cellular proteins, lipids and DNA, damaging the cell and leading to mutations (17). Furthermore, they can lead to the induction of oxidative stress, lipid peroxidation and inflammation processes (17-19). The International Agency for Research on Cancer (IARC) categorized BC as a 2B carcinogen (20). Furthermore, BC is known to cause pulmonary and cardiovascular disorders (10, 21). Accordingly, Wang *et al.* found augmented BC exposure associated with a greater increase in the progression of emphysema over a median of ten years (22). Janssen *et al.* found that reducing a unit of BC (μg/m³) exposure coming from traffic exhaust will lengthen life four to nine times more than reducing a comparable amount of PM_{2.5} mass, pinpointing how toxic BC exposure is (8).

Estimated BC emissions amount to a total of 8111 gigagrams each year (Gg/yr), with the United States and Europe contributing 321 Gg/yr and 301 Gg/yr, respectively (10). Subsequently, BC particles are omnipresent in our environment, and people are continuously exposed (8, 23). The particles infiltrate into the human body via inhalation or digestion (21). Inhaled particles with a diameter smaller than 2.5 μm can enter the lungs and pass through the lung-blood barrier, which

transfers them to the systemic circulation and eventually to various distant organs, the placenta, and the blood-brain barrier (Figure 2) (5, 8, 21, 24).

A healthy person breathes 10 – 20 m³ of air per day, depending on body constitution and physical activity (24). Pregnant women have a 20 % higher oxygen consumption and a 40-50 % increase in ventilation (24, 26). In addition, the developing fetus is extremely vulnerable to toxicant exposure due to high levels of cell proliferation, growth, and organ development (21, 24, 27). Consequently, pregnant women and their unborn children are especially vulnerable to BC exposure. Prenatal BC exposure is associated with adverse birth outcomes, such as low birth weight, intrauterine growth restriction, and altered duration of gestation in singleton pregnancies (4, 28, 29). Furthermore, studies showed an association between exposure to PM_{2.5} and BC during pregnancy and higher newborn blood pressure (30, 31). The mechanisms responsible for these altered birth outcomes concern direct and indirect pathways. Direct toxicity occurs when particles cross the placental barrier and directly interact and damage fetal tissues. Due to their high surface reactivity, particles can generate reactive oxygen species (ROS) and inflammation processes, amongst others (18). Direct effects on fetal tissues have been observed for a variety of particles in several *in vitro* and *in vivo* studies (18). However, particles can also indirectly interfere with fetal development, without direct contact with the fetus (18). The indirect pathway involves maternal and placental mediated toxicity and denotes the deposition and interaction of particles in maternal and placental tissue. Particles that interact with maternal tissues might cause the generation of ROS and eventually inflammation. Subsequently, inflammatory mediators and signaling molecules are released, which can reach the placenta or fetus and provoke toxicity. In addition, particles that reach and accumulate in the placenta also generate ROS and inflammation, thereby compromising its function and signaling processes (18, 32). Placental inflammation can reduce placental perfusion, thereby limiting nutrient and oxygen supply to the fetus, affecting fetal development (4, 29, 33). Buerki-Thurnherr *et al.* demonstrated that pulmonary exposure of pregnant mice to TiO₂ and

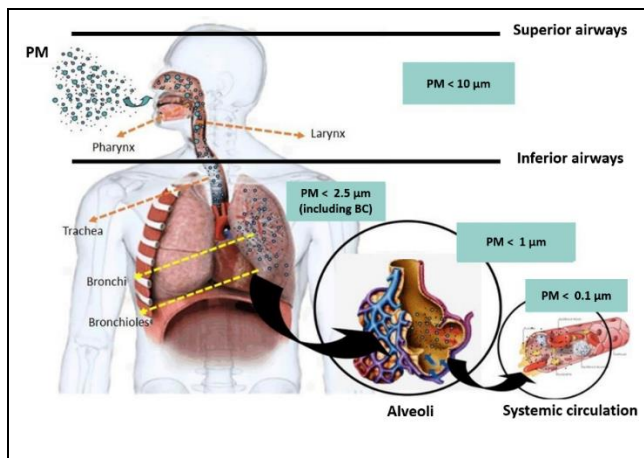


Fig. 2 – Different PM sizes and their infiltration in the human body. A mixture of PM is inhaled through the nose and enters the superior airways. PM₁₀ deposits in structures such as the nose cavity, larynx, and pharynx. PM_{2.5}, including BC particles, is able to pass on to the inferior airways via the trachea and enter lung structures such as the bronchi and bronchioli. The smallest particles (PM_{0.1}) reach and penetrate the alveoli and enter the systemic circulation. Abbreviations: PM – particulate matter, BC – black carbon, μm - micrometer. Source: figure was adapted from Castelo *et al.*, 2017 (25).

CeO₂ nanoparticles (NP) induced fetal growth restriction in the offspring without detectable particles in fetal tissue (32). These prenatal exposures are known to program the fetus for increased health risks in later life, a phenomenon known as the Developmental Origins of Health and Disease (DOHaD) (24, 34). Thereof, prenatal air pollution exposure was highlighted as a stimulus for the early programming of asthma and allergy (27). Martens *et al.* showed that an increase of 5 μg/m³ in PM_{2.5} exposure during pregnancy resulted in shorter telomeres in both cord blood and placenta, predisposing the child for accelerated biological aging in later life (35).

The placenta, a multi-layered maternal-fetal organ, is a temporary structure that provides a natural barrier between mother and child and fulfills a plethora of essential and critical functions (36-39). Its main functions consist of providing the fetus with oxygen and nutrients (*e.g.*, amino acids, carbohydrates, vitamins) and removing waste products (*e.g.*, carbon dioxide) (36, 37). Exchange of these substances occurs at the top of villous structures, located in the intervillous space (Figure 3A) (36). Maternal blood enters the intervillous space via spiral endometrial arteries, soaks the villi and drains back via endometrial veins. Oxygen

deficient fetal blood enters via the umbilical and chorionic arteries in the villi. After the exchange, oxygenated fetal blood returns via the chorionic and umbilical veins back to the fetus (36). The maternal blood in the villi is divided from the fetal blood by four distinct cell layers. Syncytiotrophoblasts, cytotrophoblasts, connective tissue of the villus, and endothelium cells lining the fetal capillaries (Figure 3B) (36, 38). Aside from exchange processes, the placenta was thought of as an impenetrable barrier that protects the fetus against xenobiotics, such as dietary substances (*e.g.*, alcohol and medicines) and environmental substances (*e.g.*, air pollutants, infections), but also from substances of maternal origin (*e.g.*, immune and hormones) (36, 38, 40). However, evidence has opposed this idea and demonstrated that NPs could reach and even translocate across the placental barrier in *in vitro*, *ex vivo*, and *in vivo* models (41). A study by Bernal-Melendez *et al.* exposed pregnant dams to diesel exhaust particles (DEP) via inhalation from gestational day (GD) 3-27 (42). At GD 28, fetal olfactory mucosa, olfactory bulbs, and whole brains were collected. NPs were found in olfactory neurons from the olfactory mucosa and in cells in the olfactory bulb of exposed fetuses, proving that the NPs crossed the placental barrier

and reached the developing fetus (42). Another study demonstrated the presence of NPs in maternal blood, fetal blood, and trophoblast cells of exposed pregnant female rabbits to DEPs close to urban pollution levels, confirming transplacental transfer (43).

Only recently, it was shown that BC particles accumulate in human placental tissue under real-life exposure conditions. Bové *et al.* demonstrated the presence of BC particles in human placentae using femtosecond pulsed laser illumination microscopy (46). Placental tissue generates second harmonic generation (SHG) and two-photon excited autofluorescence (TPAF) signals generating from collagen type I and structures such as placental cells, elastin and red blood cells, respectively (46). Due to the particles' absorptive nature and heterogeneity, they generate white light when illuminated with a femtosecond pulsed laser. Moreover, this technique has proven efficiency in the detection of BC particles in urine (46, 47). Besides accumulation in placental tissue, Bove *et al.* demonstrated a positive correlation between residential BC exposure of the mother during pregnancy and BC load in the placenta (46). Nevertheless, it is not known yet if BC particles

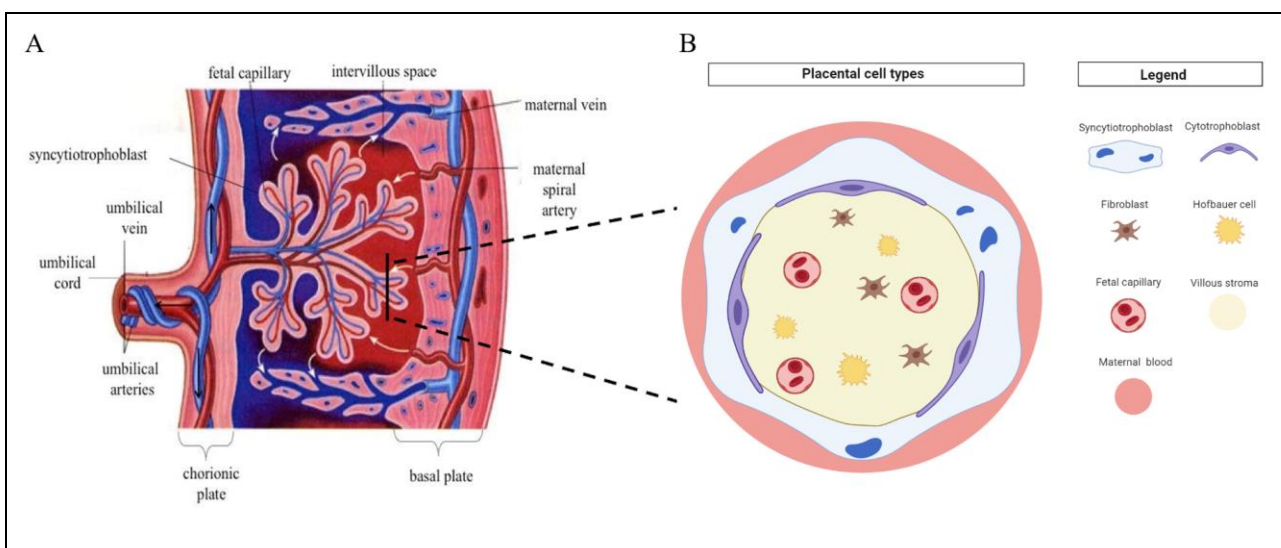


Fig. 3 – A - Part of the placental architecture and the maternal-fetal circulation. The placenta composes a maternal and a fetal unit called the basal and chorionic plate, respectively. The chorionic plate imports fetal chorionic blood vessels connected with the umbilical cord vessels, whereas the basal plate supplies the maternal blood vessels. Both plates surround the intervillous space, which encompasses villous structures containing the fetal blood vessels (36). Maternal-fetal exchange occurs at the top of these villi (36). **B** - Cross-section of a villus (as shown in figure A) with its different cell types. The maternal blood in the villi is divided from the fetal blood by four distinct cell layers; syncytiotrophoblasts (blue), cytotrophoblasts (purple), connective tissue of the villus, and endothelium cells (red) lining the fetal capillaries (36, 38). Figure B was adapted from Bongaerts *et al.* and created with Biorender.com. Source: Lofthouse *et al.*, 2014, Bongaerts *et al.*, 2021 (44, 45).

cross the human placental barrier to reach the fetal circulation. Therefore, we hypothesize that BC particles cross the placental barrier from the maternal circulation to the fetal circulation and can be detected in umbilical cord blood in humans. To explore this hypothesis, we aim to detect BC particles from ambient exposure in whole umbilical cord blood and whole maternal blood from 10 low and 10 high exposed mothers enrolled in the ENVIRONAGE (ENVIRONMENTAL influence ON Early AGEing) birth cohort. The detection of the particles will be performed by the previously mentioned microscopy technique that allows the detection of BC particles in different biological matrices as previously validated for placental tissue and urine (9). This technique offers direct visualization of the BC particles (*i.e.*, you image the particle and not fluorophores attached to the particle) without the need for sample preparation. Furthermore, particles are only identified as BC when their emission signal lies above a certain threshold and their emission ranges across the entire visible spectrum (48). In addition, the biological context is preserved, allowing for differentiation between cellular structures. Inherent to the technique are its high sensitivity and specificity (49). Detection of the BC particles in cord blood would imply exposure of the fetus to BC particles. The possible associations between ambient BC load averaged over the entire pregnancy and during the third trimester, placental BC load, maternal blood BC load, and umbilical cord blood BC load will be examined along with their presence.

In addition to the accumulation of particles in placentae, our research group detected DEPs inside three key placental cell types, *i.e.*, Hofbauer cells, endothelial cells, and trophoblasts, after *ex vivo* placental perfusion with medium containing DEPs for 6 hours (49). Trophoblasts form the outer layer of the blastocyst, providing nutrients to the embryo and develop into the main placental framework, the syncytium (38, 50). Hofbauer cells (*i.e.*, macrophages of fetal origin) reside in the placental chorionic villi and maintain a pro-angiogenic function; they manage homeostasis and morphogenesis and protect the fetus against infection (38, 51). In this regard, we will determine whether BC particles accumulate in the aforementioned placental cells after real-life human

exposure (49). A previous study demonstrated that exposure of these placental cells to PM_{2.5} (*i.e.*, PAHs and metals carried by PM_{2.5}) is thought to cause cell cycle arrest in these cells and inhibit trophoblast migration and invasion, implying placental malfunction during pregnancy (52).

This research foresees to detect BC particles in both umbilical cord blood and maternal blood from high and low exposed mothers. Moreover, it is expected that a higher residential BC exposure during pregnancy will correlate with a higher BC particle load in umbilical cord blood. Additionally, BC particles are anticipated to be internalized in specific placental resident cells. Especially trophoblasts are expected to accumulate BC particles as they are one of the first cell lineages in placental development and form the maternal-placental interface (39, 53). Furthermore, this study will add significance to epidemiological research since it will provide an internal and therefore personal measurement of exposure to BC particles from real-life BC exposure. Moreover, first time evidence will be provided for the translocation of BC particles from the mother to the unborn child, gaining insights into direct fetal exposure to BC during its most susceptible period of life. These findings can be used to form the foundation for appropriate policies to reduce BC emissions on a global scale, as there exists no specific guideline for BC emissions yet. Today's BC emission standards are included in those for PM_{2.5}, even though BC is acknowledged as the most toxic component (7). Subsequently, this study will raise awareness of the dangers of ambient air pollution in pregnant women and form a base for further research into the DOHaD phenomenon caused by environmental exposures.

EXPERIMENTAL PROCEDURES

Study design, study population and sample collection - Participants for this study were selected from the ongoing and prospective ENVIRONAGE birth cohort (2010), which enrolls mother-child pairs in the East-Limburg Hospital (Limburg, Belgium) (54). Solely women without a scheduled caesarian section are enrolled in the cohort and recruited newborns are found healthy and free from anomalies (pre- and postnatal), as confirmed by a medical doctor (30, 54). All women provide written informed consent and complete a

questionnaire in Dutch regarding alcohol and medication use, in-house environment, education, occupancy, health status, stress, smoking, lifestyle habits, residential address, physical activity and ethnicity (30, 54, 55). Information regarding neonatal sex, birth date, parity, time of delivery, birth weight and length, gestational age, method of delivery and pregnancy complications were retrieved from medical records (30, 54). The cohort adheres to the Declaration of Helsinki and is approved by the Ethics Committee of Hasselt University and the East-Limburg Hospital (30, 35).

20 mother-child pairs were selected from the cohort for this research project. Based on residential BC exposure during pregnancy and distance to a major road, these mother-child pairs are subdivided into low and high BC exposure groups. Participants were categorized as 'low' when their residential BC exposure was lower or equal to the 25th percentile (trimester 3 (0.90 $\mu\text{g}/\text{m}^3$) and whole (0.97 $\mu\text{g}/\text{m}^3$) BC exposure during pregnancy) in regard to the ENVIRONAGE birth cohort, and they lived further than 500 meters from a major road (E- and N-roads). On the contrary, 'high' was defined as a residential BC exposure higher or equal to the 75th percentile (trimester 3 (1.49 $\mu\text{g}/\text{m}^3$) and whole (1.43 $\mu\text{g}/\text{m}^3$) BC exposure during pregnancy) in regard to the ENVIRONAGE birth cohort and they lived within the proximity of 500 meters of a major road. Additionally, a selection of four placental samples was made to perform colocalization experiments. This study worked exclusively with non-smoking women.

Women donated a blood sample, umbilical cord blood, placental tissue (term placenta) and a urine sample. The collection of these samples is described elsewhere (35, 46, 54, 55). Briefly, placenta and the umbilical cords were compiled within 10 minutes after birth. Biopsies were collected from each quadrant of the fetal side of the placenta and one biopsy from the maternal side of the placenta (Supplementary, Figure S1) (35, 54). Umbilical cord blood (42 ml) was collected immediately after delivery in BD Vacutainer® plastic whole blood tubes with spray-coated K2EDTA (BD, USA) (35, 54). The maternal blood (20 ml) and urine were collected the day after birth in an EDTA tube and sterile container, respectively. Samples were preserved at -80 °C until further

analysis, except for the placenta involved in the colocalization experiments. These placenta were immediately fixated and paraffin-embedded after collection (35, 54, 55).

BC kinetics: placenta, maternal blood, umbilical cord blood and urine - Placental tissue was imaged as described by Bové *et al.* (46) and BC particles were calculated per mm^3 tissue. Umbilical cord blood, maternal blood and urine samples were thawed to room temperature and vortexed for 10 seconds. Next, the samples were aliquoted between a glass slide and coverslip, built as an imaging chamber. Capillary forces spread the sample equally over the entire chamber, upon which the imaging chamber was sealed to prevent drying. The resulting samples were imaged with a Zeiss LSM 880 META NLO (Carl Zeiss, Germany) at room temperature, where they were subjected to illumination with a femtosecond pulsed laser (150 fs, MaiTai DeepSee, USA) set to a wavelength of 810 nm. A 20x/0.8 objective (EC Plan_Neofluar, Carl Zeiss) was used. Emission was detected within the SHG (400 - 410 nm) and TPAF (450 - 650 nm) detection channels (46). Three repeats of a 10x10 tile scan (*i.e.*, 100 images) were made for each blood sample, resulting in an imaged area of 4499 x 4499 μm . Images of the urine samples were acquired with five repeats of a 3x3 tile scan (*i.e.*, 9 images), yielding an imaged area of 1349 x 1349 μm . All images were analyzed with ZEN Black 2.0 software (Carl Zeiss, Germany). The number of BC particles in each tile scan was evaluated with a peak-finding algorithm in Matlab (Matlab 2010, Mathworks, The Netherlands), which counts pixels above an experimentally determined intensity threshold. Particles identified as BC when their emission signal was present in both channels (SHG and TPAF) and the intensity of emitted white light exceeded the threshold value, given in an output figure (Supplementary, Figure S2). Based on the number of particles in the imaging volume, the number of particles per mL of blood or urine was calculated. Additionally, urine osmolality was analyzed with the K-7400S semi-micro osmometer (Knauer, Germany).

BC biodistribution: Colocalization experiments - The general placental structure was analyzed with a Hematoxylin-Eosin stain (Supplementary, Figure S3). The distribution of BC

particles in placental tissue was examined by staining endothelial cells, Hofbauer cells and trophoblasts as described by Bongaerts *et al.* (44). Briefly, tissues were dehydrated in increasing ethanol (EtOH) (VWR Chemicals, USA) concentrations (75-100%) and embedded in molten paraffin (62°C). After tissue embedment, 4 µm thick sections were made using a microtome (Leica Biosystems, Germany) and then processed for immunohistochemistry analysis. In short, sections were deparaffinized in xylene (Merck, Germany) and rehydrated in decreasing EtOH concentrations (100-95-80-70-50%). Heat-induced antigen retrieval was applied by incubating the samples in a 10 mM sodium citrate buffer (pH 6) at 97°C for 40 minutes. The endogenous peroxidase activity of the tissue was blocked by a 0.3% H₂O₂ solution and subsequently, sections were incubated with 100% protein block (56) for 60 minutes (Agilent DAKO, USA). Thereafter, sections were incubated overnight with monoclonal mouse anti-human CD68 clone KP1 antibody (1:100, M0814, Agilent, USA), mouse anti-human CD31 antibody (1:100, M0823, Agilent, USA) and monoclonal mouse anti-human cytokeratin EA1/EA3 antibody (1:50, N1590, Agilent, USA). Next, the conjugated secondary goat anti-mouse Alexa Fluor® 555 antibody (1:500, A2122, Invitrogen, USA) was applied to the sections for 60 minutes, followed by incubation for 7 minutes with Syto™ 61 Red fluorescent (1:1000, S11343, Invitrogen, USA) as a nuclear counterstain. Between every step, sections were washed with phosphate buffered saline (PBS). All antibodies were diluted in 10% PB-PBS. Sections were stained in triplicate and primary, secondary and endogenous controls were included.

The stained sections were imaged with a Zeiss LSM 880 confocal microscope (Carl Zeiss, Germany). Placental cells were visualized using the 20x/0.8 objective (Plan-Apochromat, Carl Zeiss). Alexa Fluor® 555-labeled placental cells were visualized with a 543 He-Ne laser and the counterstain Syto™ 61 Red was visualized with a 633 He-Ne laser. BC particles were detected as previously described. Three repeats of 3x3 tile scans were made per placental section (*i.e.*, three locations/section) and nine sections per ID were screened. All images were achieved by ZEN Black 2.0 software (Carl Zeiss, Germany). To quantify the colocalization of BC with the placental cells,

Mander's overlap coefficients were determined by the open source software Fiji, using Just Another Colocalization Plugin (JACoP) (Image J v 1.53i) (57).

Residential BC exposure - The residential BC exposure (µg/m³) was determined with a validated spatiotemporal interpolation method incorporating regional and local air pollution aspects in Flanders (58). Satellite images that generate land cover data (CORINE landcover data set) and pollution data of multiple official fixed monitoring stations are used to estimate hourly pollutant concentrations in a 4x4 km² receptor grid (54, 58, 59). Hence, daily exposure values are provided by combining the interpolation method with a dispersion model using emissions from line sources, point sources and Belgian telemetric air quality networks (54, 58, 59). Additionally, distance to a major road (500 meters) (E- and N-roads) and traffic density were two traffic indicators taken into account, using the Geographic Information System (ArcGIS 10 software) (54). Maternal BC exposure was already calculated and available for each trimester, last week/month/year of pregnancy, and the entire pregnancy. Address changes during pregnancy were considered.

Statistical analysis - Statistical analysis was performed with R-studio version 3.6.2 (2019) © and GraphPad Prism 9.1.0 software (60, 61). Continuous variables are expressed as mean ± standard deviation (SD), categorical variables are expressed as number and percentage (%). Data were logarithmically transformed to meet the assumptions for normality and homoscedasticity. Groups of high and low exposure were compared using a Student t-test (Welch's correction) or Mann-Whitney test. Furthermore, the correlation was determined by calculating the Pearson correlation coefficient to look for associations between modelled BC exposure and BC load in the different biological matrices (*i.e.*, blood, urine and placenta). Multiple regression analysis was performed to look at associations between BC load in blood and covariates. In the biodistribution analysis, Mander's coefficients were calculated and a one-way ANOVA with post-hoc Tukey Multiple Comparisons test was adopted to compare the BC load between the different placental cell types. Significance was assessed at 5%.

RESULTS

Study population characteristics – The study population of this research comprised 20 mother-child pairs from the ENVIRONAGE birth cohort. Based on the BC levels at the mothers’ residence and distance to a major road, mothers were classified as being exposed to low BC levels (n = 10) or high BC levels (n=10) during pregnancy. The average BC exposure measured over the entire pregnancy was 0.97 µg/m³ and 1.43 µg/m³ for the

low and high exposed mothers, respectively. Characteristics of the study population are shown in table 1. Briefly, neonates had an average birth weight of 3444.45 gram and measured 50.02 centimeter. 55% of the studied neonates were male and 75% was European. Mothers delivered at the mean age of 30.55 years old and all of them gave already birth to at least one child. The average duration of gestation was 278.85 days. 55% of the selected mothers had a high education (college or

Table 1 – Characteristics of the ENVIRONAGE study population.

<u>Neonatal characteristics</u>	Low exposure (n=10)	High exposure (n=10)	Total (n=20)	P-value
Birth weight (g)	3261.40 ± 478.14	3627.50 ± 459.62	3444.45 ± 493.59	P = 0.0979
Birth length (cm)	49.28 ± 28	50.75 ± 1.70	50.02 ± 2.36	P = 0.1687
Gender - Boy	5 (50%)	6 (60%)	11 (55%)	P > 0.9999
Ethnicity - European	8 (80%)	7 (70%)	15 (75%)	P > 0.9999
<u>Maternal characteristics</u>	Low exposure (n=10)	High exposure (n=10)	Total (n=20)	P-value
Age	29.20 ± 4.18	31.90 ± 4.53	30.55 ± 4.47	P = 0.1833
Education				P = 0.7915
Low	1 (10%)	3 (30%)	4 (20%)	
Middle	4 (40%)	1 (10%)	5 (25%)	
High	5 (50%)	6 (60%)	11 (55%)	
Ever smoked before	0 (0%)	0 (0%)	0 (0%)	NA
Parity				P = 0.1815
1 child	4 (40%)	3 (30%)	7 (35%)	
2 children	5 (50%)	4 (40%)	9 (45%)	
>3 children	1 (10%)	3 (30%)	4 (20%)	
Duration of gestation (days)	278.60 ± 8.57	279.10 ± 6.56	278.85 ± 7.43	P = 0.8851
Season of delivery				P = 0.1460
Winter	2 (20%)	4 (40%)	6 (30%)	
Spring	3 (30%)	5 (50%)	8 (40%)	
Summer	3 (30%)	0 (0%)	3 (15%)	
Autumn	2 (20%)	1 (10%)	3 (15%)	
BC exposure during pregnancy				
Trimester 1	0.91 ± 0,24	1.56 ± 0.39	1.23 ± 0.46	P = 0.0003
Trimester 2	0.80 ± 0.16	2.15 ± 0.53	1.48 ± 0.79	P < 0.0001
Trimester 3	0.90 ± 0.08	1.49 ± 0.29	1.29 ± 0.65	P < 0.0001
Total pregnancy	0.97 ± 0.12	1.43 ± 0.31	1.33 ± 0.58	P < 0.0001
Distance to major road (m)	1543.35 ± 407.67	169.94 ± 150.08	856.65 ± 765.36	P < 0.0001

Table 1. Characteristics of the mother-child pairs enrolled in the ENVIRONAGE birth cohort. Continuous data are shown as mean ± SD, categorical data are given as number and percentage (%). Neonatal characteristics are shown for birth weight (gram), birth length (centimeter), gender (boy) and ethnicity. Maternal characteristics comprise age (years), education, smoking history, parity, duration of gestation (days), season of delivery and BC exposure during pregnancy (µg/m³). Classification of ethnicity is based on the native country of the neonates’ grandparents as either European (two out of four grandparents were European) or non-European (at least three grandparents were of non-European origin, e.g., Turkey, Morocco, etc.). Maternal education was coded “low”, indicating the mother has no diploma or a lower education (lower secondary (1st – 3rd middle school)). Education was coded “middle”, meaning the mother has finished higher secondary education and education was classified “high”, indicating the mother has a college or university degree. History of smoking was coded as never smoked, stopped a while ago or current smoker. Parity was categorized into giving live birth to one, two or more than three children. Statistics: Student t-test (with Welch’s correction) or Mann-Whitney test. Significance at p < 0.05. The groups did not significantly differ from each other, except for BC exposure during pregnancy. Abbreviations: n – sample size, SD - standard deviation, NA – not applicable.

university degree). None of the selected women smoked or had a smoking history. No significant differences were observed for the described characteristics between the groups of low and high BC exposure, except for the BC exposure during pregnancy (Table 1).

BC kinetics: placenta, maternal blood and umbilical cord blood - To study whether BC particles cross the placental barrier, placentae, umbilical cord blood and maternal blood samples were analyzed for their BC load using LSM 880 confocal microscope. Detection of BC particles was based on the white light generation of carbonaceous particles under femtosecond pulsed laser illumination (48).

BC load was measured in placentae from both exposure groups (*i.e.*, low and high) and particles could be detected in all screened placentae. Results show an average BC load (SD) of 3.02×10^3 (3.17×10^3) particles per mm^3 in the low exposure group and 6.77×10^3 (7.35×10^3) particles per mm^3 in the high exposure group. High exposed mothers had a significant higher number of BC particles accumulated in their placenta compared to those with a low exposure ($p = 0.0164$) (Figure 4).

Next, maternal and umbilical cord blood samples of low and high exposed mothers were screened for BC particles. All screened blood samples contained BC particles. Maternal blood samples had an average BC load (SD) of 7.49×10^4 (5.64×10^4) in the low exposure group and 3.03×10^5 (2.34×10^5) in the high exposure group. The BC load in umbilical cord blood was lower and accounted 1.66×10^4 (7.24×10^3) BC particles per mL blood in low exposed mothers and 1.31×10^5 (9.98×10^4) particles per mL blood in high exposed mothers. Differences in BC load were found statistically significant between maternal and umbilical cord blood samples within the low exposed ($p = 0.0013$) and high exposed group ($p = 0.0201$) (Figure 5A). Furthermore, we looked at differences in BC load for the low and high exposed groups for both maternal and umbilical cord blood. Higher BC load was detected in maternal ($p = 0.0002$) and umbilical cord blood ($p < 0.0001$) samples for high exposed individuals (Figure 5B). No statistical significant correlations were found between BC load in umbilical cord blood and birth

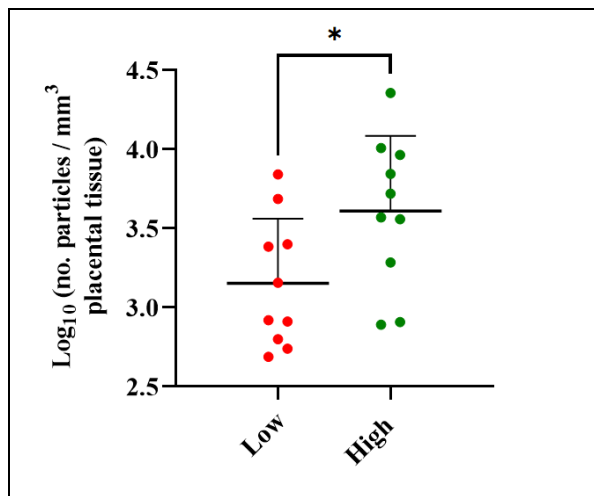


Fig. 4 – Column graph with individual points representing the BC load for placentae. Number of BC particles per mm^3 tissue for the low and high BC exposure groups. Five repeats of 3x3 tile scans were made by femtosecond pulsed laser illumination. All data are logarithmically transformed. Data are shown as mean \pm SD. Horizontal line indicates mean. A Student-test was performed * $p < 0.05$. Abbreviations: no. - number, mm^3 – cubic millimeter.

length ($p = 0.9523$), birth weight ($p = 0.2974$), duration of gestation ($p = 0.4781$) and season of delivery ($p = 0.0596$).

BC kinetics: urine - In regard of BC particles entering the maternal circulation, we measured BC load in urine samples of exposed mothers. In addition, osmolality was measured. One urine sample was not available and for one urine sample we were not able to measure osmolality, resulting in the analysis of 18 urine samples. All examined urine samples were corrected for osmolality.

BC detection in urine samples resulted in an average BC load (SD) of 6.00×10^5 (6.83×10^5) and 1.28×10^6 (2.15×10^6) particles per mL urine for the low and high exposed mothers, respectively. The high and low exposed groups did not significantly differ from each other after correction for osmolality ($p = 0.5460$). Pearson correlation coefficient showed a positive, although not significant, correlation between modelled and measured BC load ($r = 0.46$, $p = 0.0603$).

Residential BC exposure - Mothers were either categorized as low or high exposed, based on the BC levels at their residence. Maternal residential BC exposure was calculated via exposure models

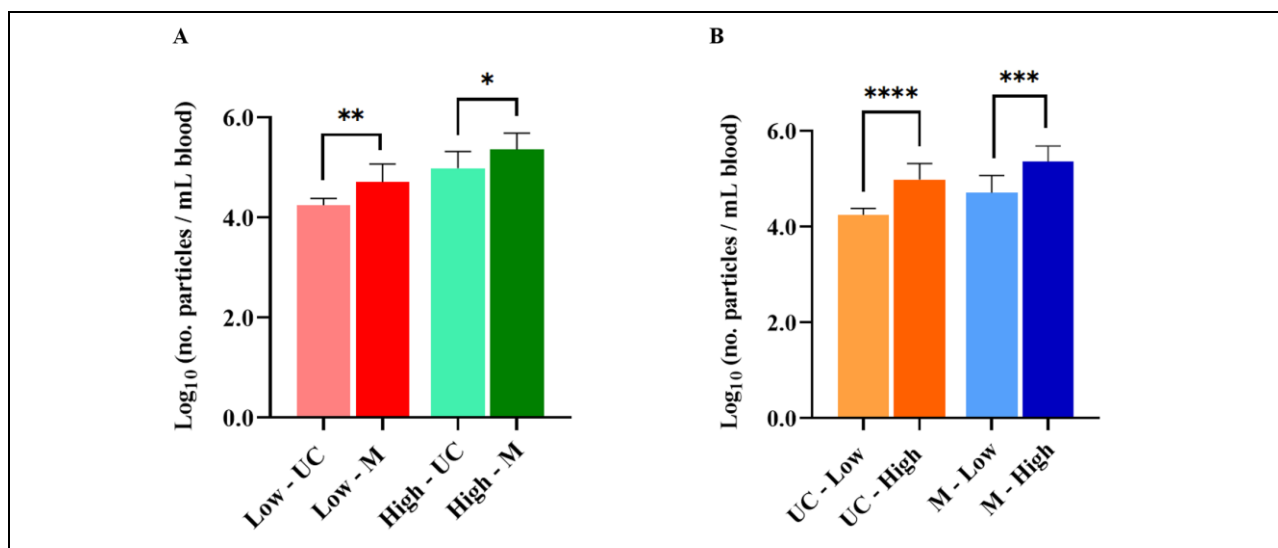


Fig. 5 – Bar plots showing BC load measured in maternal and umbilical cord blood according to residential BC exposure. **A** - Number of BC particles per mL blood for the high and low BC exposure groups, subdivided for maternal and umbilical cord blood. Three repeats of 10x10 tile scans were made. **B** - Number of BC particles measured per mL blood for maternal and umbilical cord samples, subdivided in low and high residential BC exposure. Three repeats of 10x10 tile scans were made. All data are logarithmically transformed. Data are shown as mean ± SD. A Student-test was performed. * p <0.05, ** p <0.01, *** p <0.001, **** p <0.0001. Abbreviations: UC – Umbilical cord, no. - number, mL - milliliter.

previously discussed. Low and high exposure levels were identified as BC levels measured during the third trimester and BC levels averaged over the whole pregnancy below the 25th percentile or above the 75th percentile, respectively, in regard to the entire ENVIRONAGE study population. Low exposed mothers had a residential BC load lower or equal to 0.97 µg/m³ averaged over the entire pregnancy and 0.90 µg/m³ in the last trimester of their pregnancy. In addition, they lived more than 500 meters away from a major road. On the other hand, mothers with a high residential BC load had an estimated BC exposure higher or equal to 1.43 µg/m³ averaged over their entire pregnancy and 1.49 µg/m³ in the last trimester of their pregnancy. Moreover, they lived within the proximity of 500 meters of a major road. Mothers classified as low exposed lived on average (SD) 1543 (408) meters away from a major road and mothers classified as high exposed lived 170 (150) meters from a major road.

A significant difference was observed between high and low residential BC exposure (p <0.0001) (Table 1). Pearson correlation coefficients demonstrate that residential BC exposure positively correlates with the measured BC load averaged over the entire pregnancy in placentae (r = 0.48, p

= 0.034), maternal (r = 0.66, p = 0.002) and umbilical cord blood (r = 0.90, p <0.0001) (Figure 6A). Furthermore, a positive correlation was established between placental BC load and maternal blood BC load (r =0.51, p = 0.023) and placental BC load and umbilical cord blood BC load (r = 0.56, p = 0.011). In addition, maternal and umbilical cord blood BC load showed an even higher correlation (r = 0.65, p = 0.002).

Furthermore, we looked at correlations between measured BC load in umbilical cord blood and BC exposure during the different trimesters, while correcting for the trimesters not considered (Figure 6B). Modelled BC exposure demonstrated positive correlations between measured BC load in umbilical cord blood in trimester 1 (r = 0.06, p = 0.79), trimester 2 (r = 0.70, p = 0.0009), and trimester 3 (r = 0.26, p = 0.28).

BC biodistribution: colocalization experiments - To examine the cellular biodistribution of BC particles in placental tissue, we colocalized BC particles with three native placental cell types, *i.e.*, trophoblasts (TB), endothelial cells (EC) and Hofbauer cells (HC) (Figure 8). Characteristics of the examined

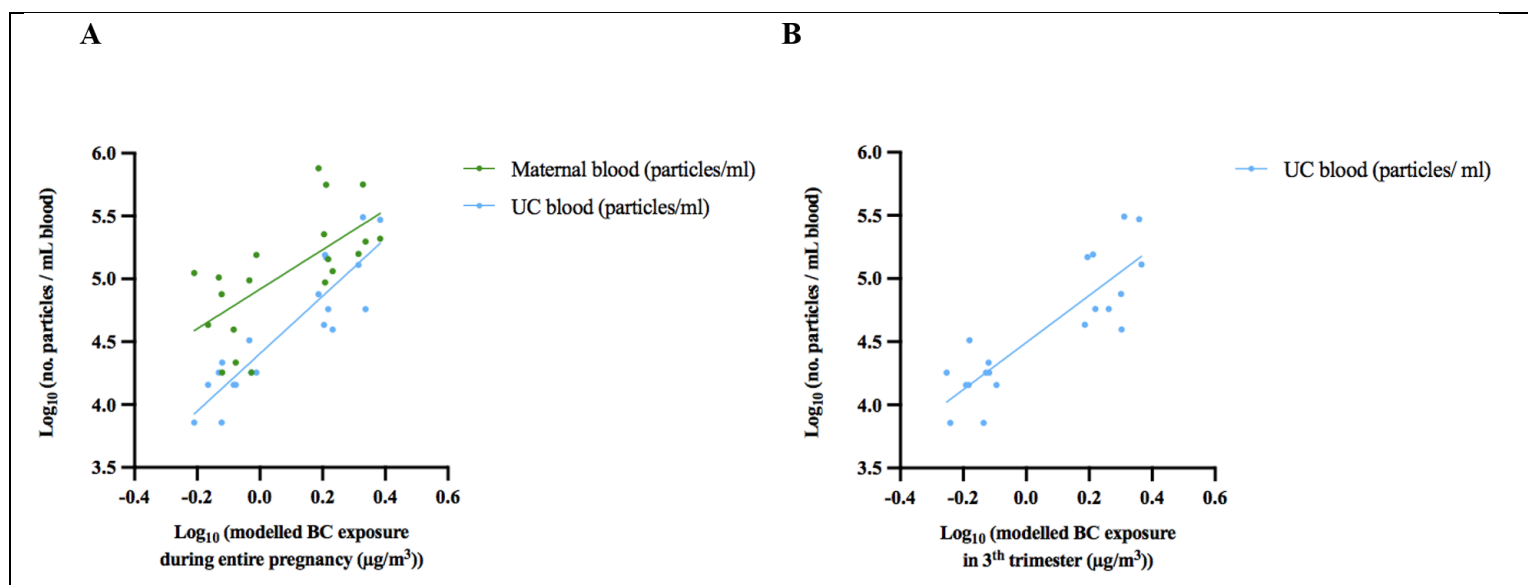


Fig. 6 – Scatterplot of residential BC levels ($\mu\text{g}/\text{m}^3$) in function of the number of measured BC particles in blood samples. **A** - Maternal blood (green) and umbilical cord blood (blue). A positive correlation was found between residential BC levels and all measured BC loads. **B** – BC load in umbilical cord blood showed a positive correlation with modelled BC exposure during the third trimester, however this correlation was not found significant. Data were logarithmically transformed. Pearson correlation coefficients were determined. Abbreviations: BC – black carbon, UC – umbilical cord, μg – microgram, mL - milliliter.

placental samples can be found in the supplementary Table S1. BC particles were

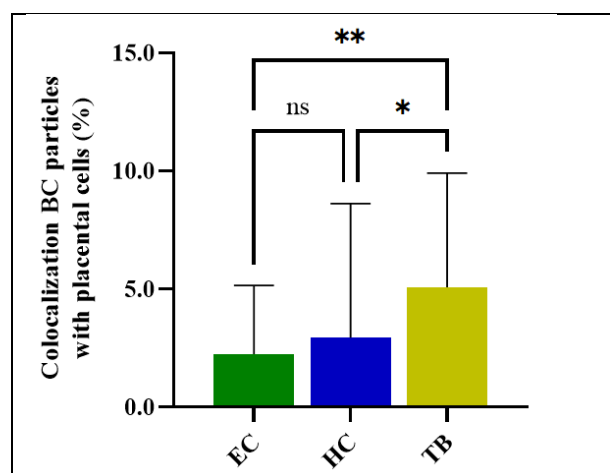


Fig. 7 – Bar plot representing the percentage of BC particles that colocalize with placental endothelial cells, Hofbauer cells and trophoblasts. BC particles were imaged under femtosecond pulsed laser illumination and Mander’s coefficients were calculated to determine percentage (%). Trophoblasts showed most accumulation of BC particles (%). No significant difference was observed between internalization of BC particles in endothelial cells and Hofbauer cells. Data represent the colocalization coefficient and SD. One-way ANOVA with post-hoc Tukey Multiple Comparisons test. * $p < 0.01$, ** $p < 0.001$. Abbreviations: EC – endothelial cells, HC – Hofbauer cells, TB – trophoblasts, BC – black carbon, ANOVA: analysis of variance, ns – not significant, SD – standard deviation.

visualized in tissue samples from four placentas with the white light generation microscopic technique. Next, we determined the percentage overlap between these placental cell types and BC particles by calculating the Manders’ overlap coefficients. This coefficient renders two percentages, M1 and M2. M1 indicates the percentage of stained cells that contain the BC particles and M2 indicates the percentage of BC particles within the stained cells.

BC particles were detected in all four screened placentae. The average BC load (SD) accounted 5.57×10^4 (9.63×10^3), 3.22×10^4 (1.44×10^4), 2.56×10^4 (1.10×10^4) and 2.78×10^4 (1.51×10^4) particles per mm^3 tissue. Moreover, we determined the percentage overlap between these placental cell types and BC particles by calculating the Manders’ overlap coefficients. Internalization was observed in all four screened samples. The mean overlap (SD) was 2.24 % (2.77) for the endothelial cells, 2.95% (3.96) for the Hofbauer cells and 5.08 % (4.84) for trophoblasts. Trophoblasts exhibited the highest accumulation of BC particles compared to endothelial cells ($p=0.0055$) and Hofbauer cells ($p=0.0280$). No difference in uptake was observed between the endothelial and the Hofbauer cells ($p > 0.9999$) (Figure 7).

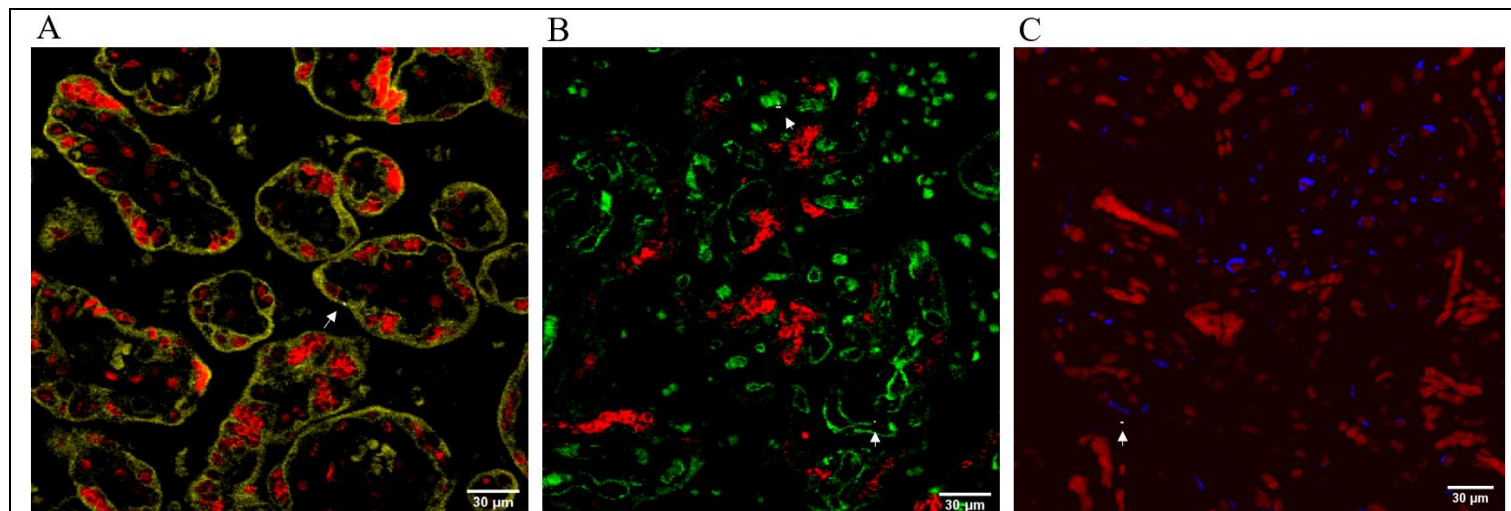


Fig. 8 - Distribution of BC particles in fresh paraformaldehyde fixed placental tissue. Images of placental sections with the stained structures of interest. **A** - Trophoblasts are stained with anti-cytokeratin (yellow). **B** - Endothelial cells are stained with anti-CD31 (green). **C** - Hofbauer cells are stained with anti-CD68 (blue). Nuclei were stained with Syto-61 Red (red) (A-C). BC particles were imaged under femtosecond pulsed laser illumination and indicated by the white arrows. Scale bar is set to 30 μm . Abbreviations: μm – micrometer.

DISCUSSION

BC kinetics: BC detection in placenta, maternal and umbilical cord blood - In the prospect that BC particles translocate from the maternal circulation towards the placenta, we screened maternal and umbilical cord blood samples for their BC load to determine whether these particles are able to cross the placental barrier and enter the fetal circulation. BC particles were detected in all analyzed placental and blood samples, demonstrating that the placenta is not an impenetrable barrier and particles in fact reach the fetal circulation. We observed a higher BC load in maternal blood compared to umbilical cord blood, indicating that BC particles reach the fetal circulation, albeit in limited amounts (Figure 5).

Our results are corresponding with previous studies that looked at the transfer of NPs and combustion-derived particles in various *ex vivo*, *in vitro* and *in vivo* models (42, 64). However, these models are not a complete representation of the real-life human situation, as the placenta is a species-specific organ and the studied models (*e.g.*, mice, rats, rabbits) have a different placental structure (*i.e.*, multiple trophoblast layers compared to one continuous layer), which makes extrapolation to the human situation difficult (32, 65, 66). Therefore, animal models are not the optimal model to study placental translocation processes. Furthermore, *ex vivo* and *in vitro* studies

often use human tissue. Wick *et al.* showed via an *ex vivo* placental perfusion model that polystyrene NPs with a diameter less than 240 nm cross the placental barrier and reach the fetal circulation (67). However, these models lack proper anatomical architecture and blood flow (65). Placental blood flow decreases during the transition from spiral arteries (*i.e.*, 70 mm Hg) towards the capillaries in the intervillous space (*i.e.*, 10 mmHg), allowing for efficient and effective perfusion of the intervillous space with maternal blood (68). Likewise, blood flow falls during the transition from the umbilical vessels (*i.e.*, 50 mm Hg) towards the villous capillaries (*i.e.*, 30 mm Hg). Subsequently, blood pressure in the umbilical vessels and their villous branches is greater than within the intervillous space, affecting transfer of substances (68). Human studies are therefore preferred and of high importance. Our research group recently demonstrated the accumulation of BC particles in human placenta and the transfer of limited amounts of DEPs through an intact placental barrier, providing evidence from real-life human exposures (44, 46).

BC particles were identified based on the white light generation when illuminated with a femtosecond pulsed laser. On the contrary, the magnitude of studies analyzing combustion derived particles used light, electron (*i.e.*, scanning and transmission), fluorescence and confocal

microscopy, often at very high magnifications (*e.g.*, x5800), to study morphological (shape, size, color, etc.) characteristics (38, 69-72). In addition, techniques such as inductively coupled plasma - mass spectrometry (ICP - MS), Brunauer - Emmett - Teller, EDX, Raman- and electron energy loss spectroscopy are applied for chemical and elemental characterization (38, 69-72). These techniques require extensive sample preparation (*i.e.*, fluorescent labeling, preparation of TEM grids, etc.), cause damage to the sample (*e.g.*, electron beam in electron microscopy) and samples are lost after analysis (*e.g.*, ICP-MS). Furthermore, visualization of particles relies on their size and shape and identification of combustion-derived particles is often a consequence of the observation of black inclusions, notwithstanding this could be other than BC particles. Correspondingly, these techniques are time consuming, expensive and lack sensitivity and specificity. Our detection technique has various advantages over aforementioned techniques. No sample preparation is required and BC particles are directly visualized (*i.e.*, you image the particle and not a fluorophore) based on their emission pattern and signal intensity (48). In addition, the biological context is preserved and samples can be measured multiple times. Detection occurs with a high specificity and sensitivity and is less time-consuming and cost-efficient in the long-term.

Residential BC exposure - Residential BC exposure was measured with a validated spatial and temporal interpolation method that provides daily exposure values for the entire pregnancy (46, 54, 58, 73). The modelled BC exposure at the mothers' residence positively correlated with the BC load measured in placentae, maternal and umbilical cord blood (Figure 6A). Furthermore, higher exposure during pregnancy resulted in a higher BC load in both maternal and umbilical cord blood. This indicates that a higher exposure leads to higher accumulation of BC in the maternal circulation, resulting in a higher fraction being transferred to the fetal circulation. Dose and duration of exposure are therefore important characteristics determining particle transfer (65). Notably, we found a higher correlation between modelled BC exposure and BC load in umbilical cord blood compared with maternal BC load. It was expected that modelled BC exposure would show a higher correlation with

maternal BC load as the mother is directly exposed to the BC particles through inhalation. This observation is remarkable and can thus far not be explained.

Additionally, a positive correlation was established between BC load in umbilical cord blood and modelled BC exposure during the different trimesters of pregnancy (Figure 6B). However, only the modelled exposure during the second trimester was found to be significantly correlated with measured BC load in umbilical cord blood. This is not what we expected, as the trophoblast layer becomes thinner towards the end of pregnancy (65). Therefore, we expected to find a significant and positive correlation between measured BC load and BC exposure in the third trimester, as translocation of substances is most convenient during this period as the placental barrier is at its thinnest (65).

These findings emphasize the need to reduce exposure of the fetus against BC particles, as we detected these particles in all examined placental and blood samples. Furthermore, we highlight the potential of BC to mediate direct toxic effects, as the developing fetus is especially vulnerable due to low levels of xenobiotic-metabolizing and detoxifying enzymes, which make tissues more sensitive to oxidative stress (74). Accordingly, this can lead to adverse birth outcomes and diseases in later life.

BC biodistribution experiments - Given the ability of BC particles to cross the placental barrier and reach the fetal circulation, we also analyzed whether these particles are internalized in key placental tissue cells, namely trophoblasts, Hofbauer cells and endothelial cells. Particles were likewise detected with the previously discussed white light detection technique under femtosecond pulsed laser illumination. Results showed accumulation in all three cell types in all examined placentae. Moreover, trophoblasts showed the highest accumulation, followed by Hofbauer and endothelial cells (Figure 7). These results align with the observations found in a study published by our research group. Bongaerts *et al.* demonstrated the accumulation of DEPs in an *ex vivo* placental perfusion model. A significant uptake of DEPs into human placental tissue after 6 hours of perfusion

was found in all three cell types. Furthermore, DEPs were detected inside fetal micro vessels (44).

Previous studies already showed that particles are taken up by trophoblasts (38, 75, 76). The high accumulation can be explained by the fact that trophoblast are the first cells to develop after implantation of the embryo, meaning they are exposed from the early beginning of pregnancy (39, 66, 77). In addition, they form a physical barrier (*i.e.*, syncytium) between maternal and fetal circulations, organized in villous structures (39, 66, 77). The continuous nature of these cells, decrease paracellular transport thereby favoring the uptake of particles in cells (44). Moreover, trophoblasts contain efflux and influx transporters on both membranes facing the maternal and fetal side, therefore, these cells can efficiently mediate maternal-fetal disposition of exogenous compounds (39). Familiari *et al.* showed via an *in vitro* approach that both PM₁₀ and PM_{2.5} are internalized by endocytosis in HTR-8/SVneo human trophoblast cells (75). Additionally, Rattanapinyopituk *et al.* demonstrated an increased number of endocytic vesicles in the cytoplasm of syncytiotrophoblasts after the administration of gold NPs to pregnant mice (78). Besides accumulation in trophoblasts, second most accumulation was observed in Hofbauer cells, which can be explained by their specialized role in the human placenta. Hofbauer cells initiate the placentas' immune response via the recognition of foreign substances. These cells act by phagocytosing these substances and secreting inflammatory cytokines (79). Multiple studies have previously shown that carbon was taken up in airway macrophages, often associated with environmental BC exposure (80-83). In addition, PM accumulation was also observed in placental macrophages, established by *in vitro* and *in vivo* approaches (38). Lastly, BC particles colocalized with placental endothelial cells, demonstrating that BC particles are in very close contact with the fetal circulation. Research already demonstrated the uptake of NPs and carbon black (CB) particles in endothelial cells via endocytosis (71, 78, 84). However, the uptake of particles depends on the prevailing shear stress and flow conditions (85).

An optimized immunofluorescence protocol was performed to visualize the cells of interest.

Placental endothelial strongly expresses CD31 in the fetal vessels (86, 87), however, Yue *et al.* showed that the expression of CD31 significantly was suppressed in mice who were exposed to PM_{2.5} towards the end of gestation (88). Therefore, alternative markers, such as anti-CD34, which showed no decreased expression when exposed to PM_{2.5} can be applied (88). The additional use of caveolin-1 has the potential to suggest endocytosis-mediated particle transfer from the maternal to the fetal circulation (78). In addition to visualizing trophoblasts with anti-cytokeratin to determine colocalization with BC particles, it would be interesting to use an additional marker for the detection of the protein clathrin. Clathrin is associated with endocytosis in syncytiotrophoblasts in mouse placenta (78). Therefore, visualization of both cytokeratin and clathrin would suggest uptake of BC particles in trophoblasts via endocytosis (78). An alternative for the visualization of Hofbauer cells are the markers CD163 and DC-SIGN, as their expression is restricted to the macrophage lineage under chorioamnionitis conditions (89).

These results demonstrate that inhaled BC particles do not only translocate to the placenta, but are also taken up in native placental tissue cells in an *in vivo*, real-life exposure condition. This has implications for the native tissue cells and indirectly towards the developing fetus. Our study did not look at possible effects of BC particles on these cells, but multiple studies have demonstrated that exposure to NP and combustion-derived particles has damaging effects on these cells. The cells may respond to the particles itself or the impurities in their surface (*e.g.*, PAHs and metals) by the induction of reactive oxygen species, autophagy and necrosis (71, 90). Furthermore, particles caused cytotoxic injury, inflammatory responses, inhibition of cell growth and apoptosis (75, 90, 91).

BC detection in maternal urine samples - In regard of BC particles entering the maternal circulation, urine samples were analyzed for their BC load. BC particles were detected in all screened urine samples, but no difference in BC load was observed between the low- and high exposed mothers. Furthermore, a positive correlation could be established between modelled BC exposure and urinary BC load. This was also demonstrated by

Saenen *et al.*, who showed that urinary black carbon load represents the accumulation of chronic exposure to combustion-related air pollution (73). In addition, these findings serve as an indication that systemic BC particles are effectively cleared from the circulation into the urine (73). Additional studies previously showed clearance of inhaled PM and BC via the kidney (73, 75). Furthermore, not only the kidneys play a role in the clearance of particles from the systemic circulation. Airway macrophages and the gastrointestinal tract are also involved in clearing inhaled PM (75, 80). A study has shown that CB particles can remain up to seven years in airway macrophages after several years of exposure in highly polluted areas. In less polluted areas, a half-life time of these particles was observed of two till four months (80). Clearance mechanisms may differ between individuals, possibly explaining the different BC load in urine samples.

Presence of BC particles into the urine implies direct exposure of the kidneys to these particles. Again, this indicates that various distant organs are a target for potential interaction and damage of these particles. In this regard, exposure to particulates can lead to chronic kidney disease and decline in renal function, further demonstrating the need for reducing current PM and BC emissions (92).

Limitations - We acknowledge some limitations of this study. First, sample sizes were small for both the BC kinetics and biodistribution experiments. Therefore, this study should be seen as a pilot study. Power calculations were performed with the statistical program G*Power (93) to determine the optimal sample size. Power was set to 0.85 and significance level to 0.05 for all sample size calculations. Effect sizes (d) were based on the mean and SD of the current pilot study. Follow-up studies should include 74 (d = 0.71) placental samples, 60 (d= 0.80) mother-newborn blood samples and up to 620 (d = 0.20) urine samples. Biodistribution experiments should be performed on 156 (d = 0.27) placental samples. Second, we were not able to determine the size of the detected BC particles, because of the diffraction limit in optical microscopy (73). Therefore, no conclusions can be made on the size of the particles that reach the fetal circulation. Size of the translocated

particles may play a role in eliciting toxicity on the exposed tissues and therefore worth considering in further research (94). Third, contamination of BC particles in the air could have occurred. By using a clean room with filtered air to handle the samples, we avoid potential external contamination of carbon particles. Fourth, the modelled BC exposure relies only on outdoor residential exposure. Nevertheless, almost 70% of women in today's society are engaged in paid employment, making it interesting to also take into account occupational BC exposures (95, 96). In addition, indoor exposures have also a major contribution to personal BC exposure. Therefore, our modelled BC exposure estimates represent an underestimation of actual BC exposure.

Future perspectives – Placental inflammation in animal models was shown to increase translocation of NPs to the fetus (97). Inflammation of the placenta is characterized by the infiltration of the placenta by maternal cells such as lymphocytes, macrophages and plasma cells (98). Inflammation can be established during pregnancy by determining leukocyte differential counts, C-reactive protein concentrations and neutrophil to lymphocyte ration. All of the aforementioned parameters are increased in women with placental inflammation. These non-invasive markers for placental inflammation have sufficient accuracy, sensitivity and specificity to assess inflammation status in pregnant women and can be performed via simple blood collection (99). In addition, inflammation can also be determined after birth. A major characteristic of placental inflammation is the infiltration of CD8 positive T-cells in placental structures. Therefore, immunofluorescence could be performed to target these cells (anti-CD8 antibodies), providing an indication whether the mother endured placental inflammation (98).

Further research is necessary to study whether translocated BC particles accumulate and target fetal tissues. However, due to ethical concerns this is very challenging. Furthermore, our birth cohort includes mother-newborn pairs at birth and performs follow-up of these children at the age 4 - 6 years old and a follow-up at the age of 10 -12 years old is now also considered. This creates the opportunity to establish possible health and developmental effects of prenatal BC exposure.

This can lead to perspectives on the direct effects of prenatal BC exposure and provide insight into the DOHaD phenomenon.

CONCLUSION

In conclusion, BC particles are present in maternal and umbilical cord blood, suggesting the translocation from the maternal circulation to the fetal circulation. Accordingly, the fetus endures direct exposure to the most toxic component of environmental particulate matter during its most susceptible period of life. Further investigation is necessary to establish the mechanism by which the transferred BC particles influence development and birth outcomes. In addition, BC particles were internalized in key placental tissue cells, including endothelial cells. Accumulation of these particles can interfere with normal cell function and eventually impair placental function and barrier integrity. We observed a positive correlation between modelled BC exposure and BC load in all examined biological samples, implying that a higher exposure result in a higher amount of particles that translocate towards various distant organs. This emphasizes the need for reducing BC emissions on a global scale.

Acknowledgements – This work was supported by Hasselt University and the Centre for Environmental Sciences. Assistance was provided by Advanced Optical Imaging Center at BIOMED. Prof. dr. Tim Nawrot is gratefully thanked for giving the opportunity to join his research group for this compelling internship. Furthermore I would like thank my supervisor miss Eva Bongaerts for all the skillful technical assistance and advice given during this internship. Miss Lintsen is thanked for her assistance during immunofluorescence experiments and miss Thessa Van Pee and Charlotte Van Der Stukken for their insights in statistical knowledge.

Author contributions – Tim Nawrot and Eva Bongaerts designed the research. Liesa Engelen performed experiments and data analysis. Eva Bongaerts provided assistance with the experiments, insights in statistical analysis and feedback on the paper.

REFERENCES

1. institute He. A special report on global exposure to air pollution and its health impacts. Boston: Health effects institute; 2020.
2. Eklund AG, Hidy GM, Watson JG, Chow JC. Public health and components of particulate matter: the changing assessment of black carbon. *J Air Waste Manag Assoc.* 2014;64(6):617-9.
3. Kilian J, Kitazawa M. The emerging risk of exposure to air pollution on cognitive decline and Alzheimer's disease - Evidence from epidemiological and animal studies. *Biomed J.* 2018;41(3):141-62.
4. Rokoff LB, Rifas-Shiman SL, Coull BA, Cardenas A, Calafat AM, Ye X, et al. Cumulative exposure to environmental pollutants during early pregnancy and reduced fetal growth: the Project Viva cohort. *Environ Health.* 2018;17(1):19.
5. Morakinyo OM, Mokgobu MI, Mukhola MS, Hunter RP. Health Outcomes of Exposure to Biological and Chemical Components of Inhalable and Respirable Particulate Matter. *Int J Environ Res Public Health.* 2016;13(6).
6. Spirina NN, Spirin NN, Dubchenco EA, Boyko AN. [Effect of different groups of first line DMT on endothelial damage in multiple sclerosis]. *Zh Nevrol Psikhiatr Im S S Korsakova.* 2020;120(7. Vyp. 2):83-8.
7. Grahame TJ, Klemm R, Schlesinger RB. Public health and components of particulate matter: the changing assessment of black carbon. *J Air Waste Manag Assoc.* 2014;64(6):620-60.
8. Janssen NA, Hoek G, Simic-Lawson M, Fischer P, van Bree L, ten Brink H, et al. Black carbon as an additional indicator of the adverse health effects of airborne particles compared with PM10 and PM2.5. *Environ Health Perspect.* 2011;119(12):1691-9.
9. Agency EE. Status of black carbon monitoring in ambient air in Europe. 2013.
10. Kucbel M, Corsaro A, Svedova B, Raclavska H, Raclavsky K, Juchelkova D. Temporal and seasonal variations of black carbon in a highly polluted European city: Apportionment of potential sources and the effect of meteorological conditions. *J Environ Manage.* 2017;203(Pt 3):1178-89.
11. Rasmussen MK, Pedersen JN, Marie R. Size and surface charge characterization of nanoparticles with a salt gradient. *Nature Communications.* 2020;11(1):2337.

12. Lindner K, Ströbele M, Schlick S, Webering S, Jenckel A, Kopf J, et al. Biological effects of carbon black nanoparticles are changed by surface coating with polycyclic aromatic hydrocarbons. *Particle and fibre toxicology*. 2017;14(1):8-.
13. Chu H, Shang J, Jin M, Chen Y, Pan Y, Li Y, et al. Comparison of lung damage in mice exposed to black carbon particles and 1,4-naphthoquinone coated black carbon particles. *Sci Total Environ*. 2017;580:572-81.
14. Paunescu AC, Casas M, Ferrero A, Panella P, Bougas N, Beydon N, et al. Associations of black carbon with lung function and airway inflammation in schoolchildren. *Environ Int*. 2019;131:104984.
15. Qian Li JS, Tong Zhu. Physicochemical characteristics and toxic effects of ozone-oxidized black carbon particles. *Atmospheric Environment*. 2013;81:68-75.
16. Ulrich P. Formation and Decomposition of Hazardous Chemical Components Contained in Atmospheric Aerosol Particles. *Journal of Aerosol Medicine*. 2002;15(2):203-12.
17. Kim KH, Jahan SA, Kabir E, Brown RJ. A review of airborne polycyclic aromatic hydrocarbons (PAHs) and their human health effects. *Environ Int*. 2013;60:71-80.
18. Dugershaw BB, Aengenheister L, Hansen SSK, Hougaard KS, Buerki-Thurnherr T. Recent insights on indirect mechanisms in developmental toxicity of nanomaterials. *Particle and Fibre Toxicology*. 2020;17(1):31.
19. Nicole AH Janssen MEG-N, Timo Lanki, Raimo O Salonen, Flemming Cassee, Gerard Hoek, Paul Fischer, Bert Brunekreef, Michal Krzyzanowsk. Health effects of black carbon. World Health Organization; 2012.
20. (IARC) IAfRoC. Agents Classified by the IARC Monographs, Volumes 1–128: IARC; 2010 [Available from: <https://monographs.iarc.who.int/list-of-classifications>].
21. Chiu YH, Bellinger DC, Coull BA, Anderson S, Barber R, Wright RO, et al. Associations between traffic-related black carbon exposure and attention in a prospective birth cohort of urban children. *Environ Health Perspect*. 2013;121(7):859-64.
22. Wang M, Aaron CP, Madrigano J, Hoffman EA, Angelini E, Yang J, et al. Association Between Long-term Exposure to Ambient Air Pollution and Change in Quantitatively Assessed Emphysema and Lung Function. *JAMA*. 2019;322(6):546-56.
23. Long CM, Nascarella MA, Valberg PA. Carbon black vs. black carbon and other airborne materials containing elemental carbon: physical and chemical distinctions. *Environ Pollut*. 2013;181:271-86.
24. Klepac P, Locatelli I, Korosec S, Kunzli N, Kukec A. Ambient air pollution and pregnancy outcomes: A comprehensive review and identification of environmental public health challenges. *Environ Res*. 2018;167:144-59.
25. Castelo FB. Human exposure assessment related to oil activities in Ecuador: from the air quality monitoring to the study of metallic contaminants transfer in the soil-plant continuum: Universite Toulouse 3 Paul Sabatier (UT3 Paul Sabatier); 2017.
26. Soma-Pillay P, Nelson-Piercy C, Tolppanen H, Mebazaa A. Physiological changes in pregnancy. *Cardiovasc J Afr*. 2016;27(2):89-94.
27. Deng Q, Lu C, Li Y, Sundell J, Dan N. Exposure to outdoor air pollution during trimesters of pregnancy and childhood asthma, allergic rhinitis, and eczema. *Environ Res*. 2016;150:119-27.
28. Bijmens EM, Derom C, Gielen M, Winkelmanns E, Fierens F, Vlietinck R, et al. Small for gestational age and exposure to particulate air pollution in the early-life environment of twins. *Environ Res*. 2016;148:39-45.
29. Kannan S, Misra DP, Dvonch JT, Krishnakumar A. Exposures to airborne particulate matter and adverse perinatal outcomes: a biologically plausible mechanistic framework for exploring potential effect modification by nutrition. *Environmental health perspectives*. 2006;114(11):1636-42.
30. Madhloum N, Nawrot TS, Gyselaers W, Roels HA, Bijmens E, Vanpoucke C, et al. Neonatal blood pressure in association with prenatal air pollution exposure, traffic, and land use indicators: An ENVIRONAGE birth cohort study. *Environ Int*. 2019;130:104853.
31. van Rossem L, Rifas-Shiman SL, Melly SJ, Kloog I, Luttmann-Gibson H, Zanobetti A, et al. Prenatal air pollution exposure and newborn blood pressure. *Environ Health Perspect*. 2015;123(4):353-9.

32. Buerki-Thurnherr T, Schaepper K, Aengenheister L, Wick P. Developmental Toxicity of Nanomaterials: Need for a Better Understanding of Indirect Effects. *Chem Res Toxicol.* 2018;31(8):641-2.
33. Ileakis JV, Tsilou E, Fisher S, Abrahams VM, Soares MJ, Cross JC, et al. Placental origins of adverse pregnancy outcomes: potential molecular targets: an Executive Workshop Summary of the Eunice Kennedy Shriver National Institute of Child Health and Human Development. *Am J Obstet Gynecol.* 2016;215(1 Suppl):S1-S46.
34. Brauer M, Lencar C, Tamburic L, Koehoorn M, Demers P, Karr C. A cohort study of traffic-related air pollution impacts on birth outcomes. *Environ Health Perspect.* 2008;116(5):680-6.
35. Martens DS, Cox B, Janssen BG, Clemente DBP, Gasparrini A, Vanpoucke C, et al. Prenatal Air Pollution and Newborns' Predisposition to Accelerated Biological Aging. *JAMA Pediatr.* 2017;171(12):1160-7.
36. Gude NM, Roberts CT, Kalionis B, King RG. Growth and function of the normal human placenta. *Thromb Res.* 2004;114(5-6):397-407.
37. Krzyzanowski A, Kwiatek M, Geca T, Stupak A, Kwasniewska A. Modern Ultrasonography of the Umbilical Cord: Prenatal Diagnosis of Umbilical Cord Abnormalities and Assessment of Fetal Wellbeing. *Med Sci Monit.* 2019;25:3170-80.
38. Liu NM, Miyashita L, Maher BA, McPhail G, Jones CJP, Barratt B, et al. Evidence for the presence of air pollution nanoparticles in placental tissue cells. *Sci Total Environ.* 2021;751:142235.
39. Staud F, Karahoda R. Trophoblast: The central unit of fetal growth, protection and programming. *The international journal of biochemistry & cell biology.* 2018;105:35-40.
40. Latendresse G, Founds S. The Fascinating and Complex Role of the Placenta in Pregnancy and Fetal Well-being. *J Midwifery Womens Health.* 2015;60(4):360-70.
41. Bongaerts E, Nawrot TS, Van Pee T, Ameloot M, Bove H. Translocation of (ultra)fine particles and nanoparticles across the placenta; a systematic review on the evidence of in vitro, ex vivo, and in vivo studies. *Part Fibre Toxicol.* 2020;17(1):56.
42. Bernal-Melendez E, Lacroix MC, Bouillaud P, Callebert J, Olivier B, Persuy MA, et al. Repeated gestational exposure to diesel engine exhaust affects the fetal olfactory system and alters olfactory-based behavior in rabbit offspring. *Part Fibre Toxicol.* 2019;16(1):5.
43. Valentino SA, Tarrade A, Aioun J, Mourier E, Richard C, Dahirel M, et al. Maternal exposure to diluted diesel engine exhaust alters placental function and induces intergenerational effects in rabbits. *Part Fibre Toxicol.* 2016;13(1):39.
44. Bongaerts E, Aengenheister L, Dugershaw BB, Manser P, Roeffaers MJB, Ameloot M, et al. Label-free detection of uptake, accumulation, and translocation of diesel exhaust particles in ex vivo perfused human placenta. *J Nanobiotechnology.* 2021;19(1):144.
45. Lofthouse EM. The accumulation of glutamate in the placental syncytiotrophoblast as a driver of membrane transport: University of Southampton; 2014.
46. Bove H, Bongaerts E, Slenders E, Bijnsens EM, Saenen ND, Gyselaers W, et al. Ambient black carbon particles reach the fetal side of human placenta. *Nat Commun.* 2019;10(1):3866.
47. Saenen ND, Bové H, Steuwe C, Roeffaers MJB, Provost EB, Lefebvre W, et al. Children's Urinary Environmental Carbon Load: A Novel Marker Reflecting Residential Ambient Air Pollution Exposure? *American Journal of Respiratory and Critical Care Medicine.* 2017;196(7):873-81.
48. Bove H, Steuwe C, Fron E, Slenders E, D'Haen J, Fujita Y, et al. Biocompatible Label-Free Detection of Carbon Black Particles by Femtosecond Pulsed Laser Microscopy. *Nano Lett.* 2016;16(5):3173-8.
49. Eva Bongaerts LA, Battuja B. Dugershaw, Pius Manser, Maarten B.J. Roeffaers, Marcel Ameloot, Tim S. Nawrot, Hannelore Bové, Tina Buerki-Thurnherr. Label-Free Detection of Uptake, Accumulation and Translocation of Diesel Exhaust Particles in the Ex Vivo Perfused Human Placenta. In: Centre for Environmental Sciences LfP-BI, editor. 2020. p. 34.
50. Wang Y ZSV. Chapter 4, Cell Types of the Placenta. *Vascular Biology of the Placenta.* San Rafael (CA): Morgan & Claypool Life Sciences; 2010.
51. Reyes L, Golos TG. Hofbauer Cells: Their Role in Healthy and Complicated Pregnancy. *Front Immunol.* 2018;9:2628.

52. Erlandsson L, Lindgren R, Naav A, Kraiss AM, Strandberg B, Lundh T, et al. Exposure to wood smoke particles leads to inflammation, disrupted proliferation and damage to cellular structures in a human first trimester trophoblast cell line. *Environ Pollut*. 2020;264:114790.
53. Roland CS, Hu J, Ren CE, Chen H, Li J, Varvoutis MS, et al. Morphological changes of placental syncytium and their implications for the pathogenesis of preeclampsia. *Cell Mol Life Sci*. 2016;73(2):365-76.
54. Janssen BG, Madhloum N, Gyselaers W, Bijmens E, Clemente DB, Cox B, et al. Cohort profile: the ENVIRONmental influence ON early AGEing (ENVIR ON AGE): a birth cohort study. *International journal of epidemiology*. 2017;46(5):1386-7m.
55. Monien BH, Abraham K, Nawrot TS, Hogervorst JGF. Levels of the hemoglobin adduct N-(2,3-Dihydroxypropyl)-valine in cord and maternal blood: Prenatal transfer of glycidol in the ENVIRONAGE birth cohort. *Toxicol Lett*. 2020;332:82-7.
56. Brahmajothi MV, Campbell DL, Rasmusson RL, Morales MJ, Trimmer JS, Nerbonne JM, et al. Distinct transient outward potassium current (Ito) phenotypes and distribution of fast-inactivating potassium channel alpha subunits in ferret left ventricular myocytes. *J Gen Physiol*. 1999;113(4):581-600.
57. Instrumentation NIOHEHLFOAC. Image Processing and Analysis in Java (ImageJ). Version 1.53i ed2021.
58. Janssen S, Dumont G, Fierens F, Mensink C. Spatial interpolation of air pollution measurements using CORINE land cover data. *Atmospheric Environment*. 2008;42(20):4884-903.
59. Lefebvre W, Degrawe B, Beckx C, Vanhulsel M, Kochan B, Bellemans T, et al. Presentation and evaluation of an integrated model chain to respond to traffic-and health-related policy questions. *Environmental modelling & software*. 2013;40:160-70.
60. GraphPad. Outlier Calculator. GraphPad Software; 2021.
61. R studio. 3.6.2 - Dark and Stormy Night ed. Boston, MA, USA2019.
62. Mohrig JR, Carlson HK, Coughlin JM, Hofmeister GE, McMartin LA, Rowley EG, et al. Novel syn intramolecular pathway in base-catalyzed 1,2-elimination reactions of beta-acetoxy esters. *J Org Chem*. 2007;72(3):793-8.
63. Khaitov RM, Pinegin BV, Pashchenkov MV. [Significance of the functional activity of toll-like receptors and other receptors of the innate immune system of the kidney physiology]. *Russ Fiziol Zh Im I M Sechenova*. 2007;93(5):505-20.
64. Vidmar J, Loeschner K, Correia M, Larsen EH, Manser P, Wichser A, et al. Translocation of silver nanoparticles in the ex vivo human placenta perfusion model characterized by single particle ICP-MS. *Nanoscale*. 2018;10(25):11980-91.
65. Buerki-Thurnherr T, von Mandach U, Wick P. Knocking at the door of the unborn child: engineered nanoparticles at the human placental barrier. *Swiss medical weekly*. 2012;142:w13559.
66. Chuva de Sousa Lopes SM, Alexdotir MS, Valdimarsdottir G. The TGFbeta Family in Human Placental Development at the Fetal-Maternal Interface. *Biomolecules*. 2020;10(3).
67. Wick P, Malek A, Manser P, Meili D, Maeder-Althaus X, Diener L, et al. Barrier capacity of human placenta for nanosized materials. *Environ Health Perspect*. 2010;118(3):432-6.
68. Wang Y ZS. *Vascular Biology of the Placenta*. San Rafael (CA): Morgan & Claypool Life Sciences; 2010.
69. Barosova H, Dvorackova J, Motyka O, Kutlakova KM, Peikertova P, Rak J, et al. Metal-based particles in human amniotic fluids of fetuses with normal karyotype and congenital malformation--a pilot study. *Environ Sci Pollut Res Int*. 2015;22(10):7582-9.
70. Bunn HJ, Dinsdale D, Smith T, Grigg J. Ultrafine particles in alveolar macrophages from normal children. *Thorax*. 2001;56(12):932-4.
71. Vesterdal LK, Mikkelsen L, Folkmann JK, Sheykhzade M, Cao Y, Roursgaard M, et al. Carbon black nanoparticles and vascular dysfunction in cultured endothelial cells and artery segments. *Toxicology Letters*. 2012;214(1):19-26.
72. Zhang R, Dai Y, Zhang X, Niu Y, Meng T, Li Y, et al. Reduced pulmonary function and increased pro-inflammatory cytokines in nanoscale carbon black-exposed workers. *Part Fibre Toxicol*. 2014;11:73.
73. Saenen ND, Bove H, Steuwe C, Roeffaers MJB, Provost EB, Lefebvre W, et al. Children's Urinary Environmental Carbon Load. A Novel Marker Reflecting Residential Ambient Air

- Pollution Exposure? *Am J Respir Crit Care Med.* 2017;196(7):873-81.
74. Campagnolo L, Hougaard K, editors. *Reproduction and Development* 2017.
75. Familiarì M, Naav A, Erlandsson L, de Jongh RU, Isaxon C, Strandberg B, et al. Exposure of trophoblast cells to fine particulate matter air pollution leads to growth inhibition, inflammation and ER stress. *PLoS One.* 2019;14(7):e0218799.
76. Kaiglova A, Reichrtova E, Adamcakova A, Wsolova L. Lactate dehydrogenase activity in human placenta following exposure to environmental pollutants. *Physiol Res.* 2001;50(5):525-8.
77. Lunghi L, Ferretti ME, Medici S, Biondi C, Vesce F. Control of human trophoblast function. *Reprod Biol Endocrinol.* 2007;5:6.
78. Rattanapinyopituk K, Shimada A, Morita T, Sakurai M, Asano A, Hasegawa T, et al. Demonstration of the clathrin- and caveolin-mediated endocytosis at the maternal-fetal barrier in mouse placenta after intravenous administration of gold nanoparticles. *J Vet Med Sci.* 2014;76(3):377-87.
79. Ozinsky A, Underhill DM, Fontenot JD, Hajjar AM, Smith KD, Wilson CB, et al. The repertoire for pattern recognition of pathogens by the innate immune system is defined by cooperation between toll-like receptors. *Proc Natl Acad Sci U S A.* 2000;97(25):13766-71.
80. Cheng W, Liu Y, Tang J, Duan H, Wei X, Zhang X, et al. Carbon content in airway macrophages and genomic instability in Chinese carbon black packers. *Arch Toxicol.* 2020;94(3):761-71.
81. Nwokoro C, Ewin C, Harrison C, Ibrahim M, Dundas I, Dickson I, et al. Cycling to work in London and inhaled dose of black carbon. *Eur Respir J.* 2012;40(5):1091-7.
82. Padovan MG, Whitehouse A, Gouveia N, Habermann M, Grigg J. Carbonaceous particulate matter on the lung surface from adults living in Sao Paulo, Brazil. *PLoS One.* 2017;12(11):e0188237.
83. Tejwani V, Moughames E, Suresh K, Tang SE, Mair LG, Romero K, et al. Black Carbon Content in Airway Macrophages is Associated with Reduced CD80 Expression and Increased Exacerbations in Former Smokers With COPD. *Chronic Obstr Pulm Dis.* 2021;8(1).
84. Samuel SP, Jain N, O'Dowd F, Paul T, Kashanin D, Gerard VA, et al. Multifactorial determinants that govern nanoparticle uptake by human endothelial cells under flow. *Int J Nanomedicine.* 2012;7:2943-56.
85. Klingberg H, Loft S, Oddershede LB, Moller P. The influence of flow, shear stress and adhesion molecule targeting on gold nanoparticle uptake in human endothelial cells. *Nanoscale.* 2015;7(26):11409-19.
86. Dye JF, Jablenska R, Donnelly JL, Lawrence L, Leach L, Clark P, et al. Phenotype of the endothelium in the human term placenta. *Placenta.* 2001;22(1):32-43.
87. Patel J, Seppanen E, Chong MS, Yeo JS, Teo EY, Chan JK, et al. Prospective surface marker-based isolation and expansion of fetal endothelial colony-forming cells from human term placenta. *Stem Cells Transl Med.* 2013;2(11):839-47.
88. Yue H, Ji X, Zhang Y, Li G, Sang N. Gestational exposure to PM2.5 impairs vascularization of the placenta. *Sci Total Environ.* 2019;665:153-61.
89. Yang SW, Cho EH, Choi SY, Lee YK, Park JH, Kim MK, et al. DC-SIGN expression in Hofbauer cells may play an important role in immune tolerance in fetal chorionic villi during the development of preeclampsia. *J Reprod Immunol.* 2017;124:30-7.
90. Yamawaki H, Iwai N. Mechanisms underlying nano-sized air-pollution-mediated progression of atherosclerosis: carbon black causes cytotoxic injury/inflammation and inhibits cell growth in vascular endothelial cells. *Circ J.* 2006;70(1):129-40.
91. Huang JP, Hsieh PC, Chen CY, Wang TY, Chen PC, Liu CC, et al. Nanoparticles can cross mouse placenta and induce trophoblast apoptosis. *Placenta.* 2015;36(12):1433-41.
92. Wu MY, Lo WC, Chao CT, Wu MS, Chiang CK. Association between air pollutants and development of chronic kidney disease: A systematic review and meta-analysis. *Sci Total Environ.* 2020;706:135522.
93. Faul Frans EE, Lang Albert, Lang George, Buchner Axel. *G * Power 3: Een flexibel programma voor statistische poweranalyse voor de sociale, gedrags- en biomedische wetenschappen.* 3.1.9.6 ed. Germany: Universität Kiel; 2007.
94. Keelan JA. Nanotoxicology: nanoparticles versus the placenta. *Nat Nanotechnol.* 2011;6(5):263-4.

95. Esteban Ortiz-Ospina ST, Max Roser. Women's employment OurWorldInData.org; 2018 [Available from: <https://ourworldindata.org/female-labor-supply>].
96. schildberg-Hörisch H. Parental employment and children's academic achievement. *Psychology*. 2016.
97. Tian X, Zhu M, Du L, Wang J, Fan Z, Liu J, et al. Intrauterine inflammation increases materno-fetal transfer of gold nanoparticles in a size-dependent manner in murine pregnancy. *Small*. 2013;9(14):2432-9.
98. Kim CJ, Romero R, Chaemsaitong P, Kim J-S. Chronic inflammation of the placenta: definition, classification, pathogenesis, and clinical significance. *American journal of obstetrics and gynecology*. 2015;213(4 Suppl):S53-S69.
99. Kim M-A, Lee YS, Seo K. Assessment of predictive markers for placental inflammatory response in preterm births. *PloS one*. 2014;9(10):e107880-e.

SUPPLEMENTARY

Table of content

Sampling of placental tissue..... 22

Overview of the protocol for detection of BC particles in blood samples 23

Determination of number of repeats..... 24

Colocalization experiments 25

 Characteristics of the placenta..... 25

 Protocol 25

 Hematoxylin-Eosin staining of placental tissue 26

S1. Sampling of placental tissue

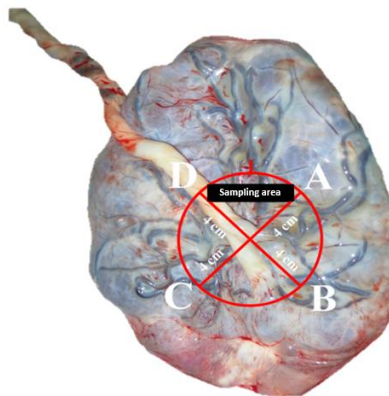


Fig. S1. Sampling scheme for placental tissue. The placenta is faced upwards and four fetal sided biopsies are taken from each quadrant (A-D) and one maternal sided biopsy is acquired, corresponding with fetal sided biopsy A. Biopsies are taken 4 cm away from the umbilical cord and 1.5 cm underneath the chorio-amniotic membrane. Source: adapted from Janssen *et al.*, 2014 (52).

S2. Overview of the protocol for detection of BC particles in blood samples

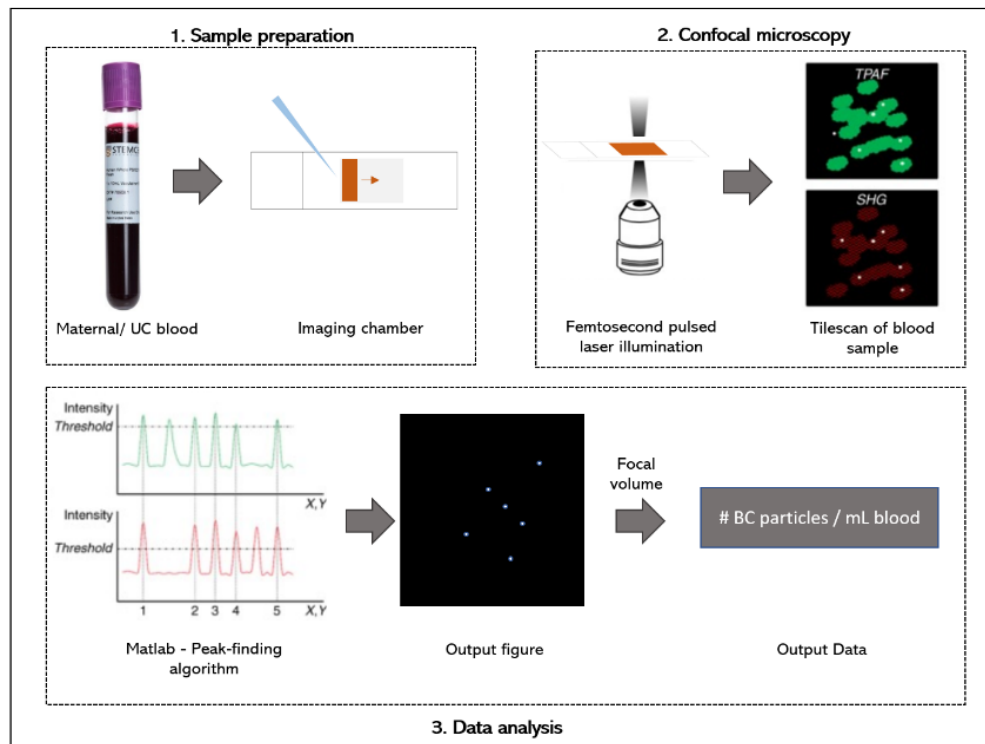


Fig. S2. Schematic representation of the experimental procedures for detection of BC particles in blood samples with femtosecond pulsed laser illumination. Sample preparation. Blood samples are aliquoted between a glass slide and a cover slip, built as an imaging chamber. Capillary forces spread the sample equally over the entire chamber. Confocal microscopy. The resulting samples are subjected to illumination with a femtosecond pulsed laser and imaged with a confocal microscope. Emission is detected within the SHG (400 - 410 nm) and TPAF (450 - 650 nm) detection channels. The imaged area is recorded as tile scans. Data analysis. The number of BC particles in each tile scan is evaluated using a peak-finding algorithm in Matlab (Matlab 2010, MathWorks, The Netherlands). Matlab software counts pixels above an experimentally determined intensity threshold. Particles identify as BC when their emission signal is present in both channels (SHG and TPAF) and the intensity of emitted white light lies above the threshold value. Based on the number of particles per imaging volume, the number of particles per mL is calculated. Source: figure was adapted from Bové *et al.* (44).

S3. Determination of number of repeats

To determine the type and number of repeats of tile scans to achieve reproducible results for each blood sample, we spiked whole adult blood samples with conductive carbon black (CCB) particles. A concentration range of 0.039 – 40 µg CCB particles per mL blood was applied.

First we looked at the variance between 3x3 and 10x10 tile scans regarding the measured number of CCB particles. Therefore, we calculated the coefficient of variation for a 3x3 and 10x10 tile scan for the spiked blood samples. Results showed a lot of fluctuations and were therefore ambiguous. However, we choose to work with 10x10 tile scans as a bigger surface is screened. Furthermore, we looked whether there was a difference in measurements when five or three tile scans (repeats) were made for blood samples. Bland-Altman plots revealed no significant differences between five or three repeats, except for the highest CCB concentration (*i.e.*, 40 µg/mL) (Figure S3A). However, 95 % of our measurements are within the limits of agreement and therefore, no difference in measured CCB load is observed when five or three repeats are considered. Furthermore, results showed a high correlation between the concentration of CCB particles and measured CCB load in blood for confocal microscope LSM 880 ($r = 0.9426$, $p < 0.0001$) (Figure S3B).

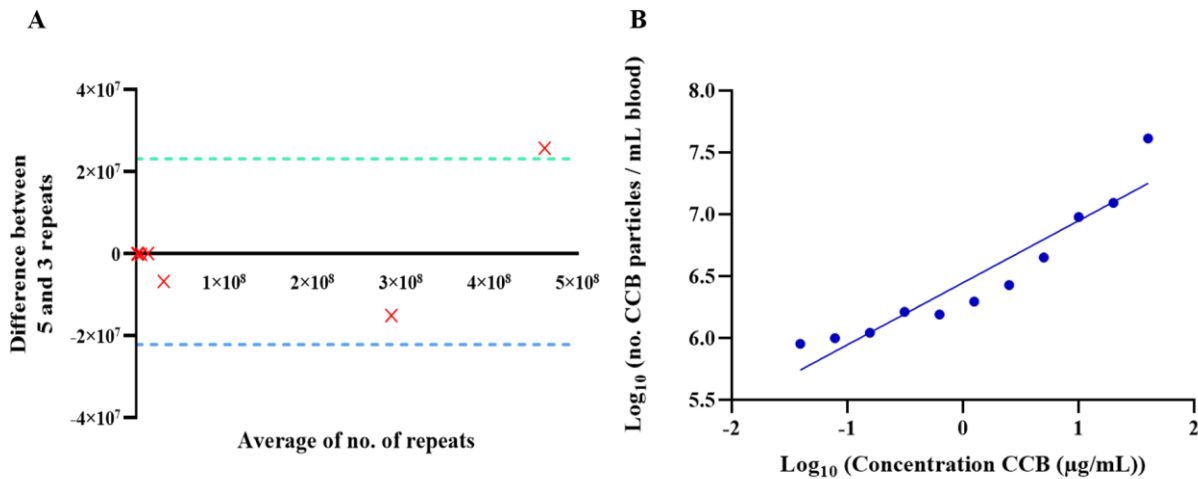


Fig. S3. **A** - Bland-Altman plot showing the difference in CCB load between five and three repeats of 10 x 10 tile scans. Green and blue dotted line represent the upper and lower limit of agreement, respectively. Red crosses represent the average of the measured CCB particles for the repeats, with five repeats being the reference. **B** – Scatterplot showing the correlation between the spiked CCB concentrations and the measured CCB load in whole adult blood. Data were logarithmically transformed. Mean values are shown. Pearson correlations were determined between spiked CCB concentration and measured CCB load in whole adult blood. Abbreviations: CCB – conductive carbon black, no. – number, µg – microgram, mL – milliliter.

S4. Colocalization experiments

S4.1. Characteristics of the studies placentae

Table S1 - Characteristics of the placental samples included in the biodistribution experiments.

	Placenta 1	Placenta 2	Placenta 3	Placenta 4
Age mother	32	29	30	28
Education	high	middle	high	low
Ever smoked before	no	no	no	no
Parity	2	1	2	2
Duration of gestation (days)	280	251	286	276
Season of delivery	winter	winter	winter	winter
BC exposure during pregnancy				
Trimester 1	0.96	1.20	0.78	0.74
Trimester 2	1.41	1.69	1.14	1.07
Trimester 3	1.58	1.55	1.26	1.07
Total pregnancy	1.31	1.47	1.05	0.96

Table S1. Characteristics of the placental samples from the ENVIRONAGE birth cohort. Placental characteristics comprise of the mother (years), education, smoking history, parity, duration of gestation (days), season of delivery and BC exposure during pregnancy ($\mu\text{g}/\text{m}^3$). Maternal education was coded “low”, indicating the mother has no diploma or a lower education (lower secondary (1st – 3rd middle school)). Education was coded “middle”, meaning the mother has finished higher secondary education and education was classified “high”, indicating the mother has a college or university degree. History of smoking was coded as never smoked, stopped a while ago or current smoker. Parity was categorized into giving live birth to one, two or more than three children.

S4.2. Protocol

Colocalization experiments were performed on one fetal-sided placental biopsy as it was previously shown by Bové *et al.* that no difference in BC load exists between different placental biopsies (46). Fresh placental biopsies were immediately fixated in 4% paraformaldehyde (Sigma-Aldrich, USA) and kept on ice for 24 hours. Tissues were then dehydrated in increasing ethanol (EtOH) (VWR Chemicals, USA) concentrations (75-100%) and afterwards embedded in molten paraffin (62°C). After tissue embedment, 4 μm thick sections were made using a microtome (Leica Biosystems, Germany). Subsequently, these sections were processed for immunohistochemistry. Briefly, the sections are deparaffinized in xylene (Merck, Germany) (2x5 min) and rehydrated in decreasing EtOH concentrations (2x5 min - 100% and 1x5 min - 95-80-70-50%), followed by washing with deionized water (1x5 min). Heat-induced antigen retrieval is applied by incubating the samples in 10 mM sodium citrate buffer (pH 6) in a 97°C water bath (Thermo Fisher Scientific, USA) for 40 minutes. Afterwards, the samples are cooled down to room temperature (30 min) and washed with phosphate buffered saline (PBS) (2x5 min) on a shaker (Fisher Scientific, USA). The endogenous peroxidase activity of the tissue is blocked by a 0.3% H_2O_2 solution (1x10 min), pursued by washing in PBS (2x5 min) and deionized water (1x5 min). Subsequently, sections are incubated with 100% protein block (56) for 60 minutes (Agilent DAKO, USA), followed by incubation overnight in a humid chamber (4°C) with the primary antibody diluted in 10% PB-PBS. The primary antibodies used for this experiment are the monoclonal mouse anti-human CD68 clone KP1 antibody (M0814, Agilent, USA) (1:100), mouse anti-human CD31 antibody (M0823, Agilent, USA) (1:100) and primary monoclonal mouse anti-human cytokeratin EA1/EA3 antibody (N1590, Agilent, USA) (1:50). Next, sections are incubated for 60 minutes with the conjugated secondary goat anti-mouse Alexa Fluor® 555 antibody (A2122, Invitrogen, USA) (1:500) diluted in 10% PB-PBS in a humid chamber. After washing with PBS (3x5 min), sections are incubated in a humid chamber (10 min) with Syto™ 61 Red fluorescent (S11343, Invitrogen, USA) diluted in 10% PB-PBS (1:1000) as a nuclear counterstain. Both primary and secondary controls were included.

S4.3. Hematoxylin-Eosin staining of placental tissue

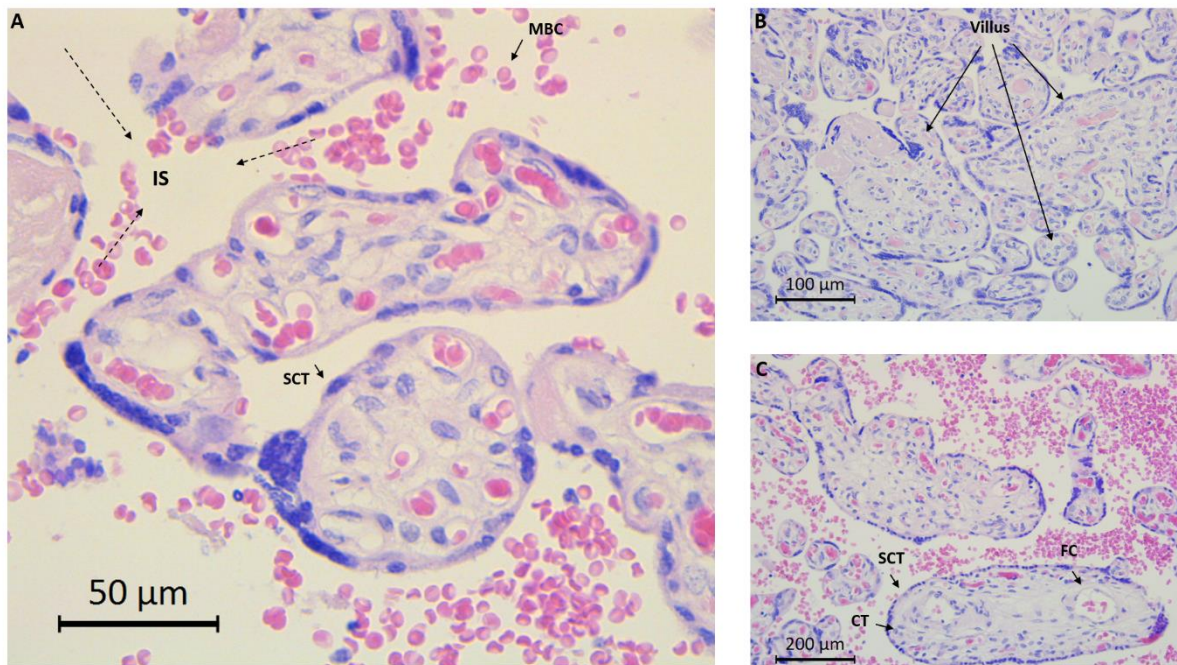


Fig. S4. Villous structures in placental tissue. Placental sections were stained with a Hematoxylin-Eosin staining to visualize the main placental architecture. **A** – Image acquired at 40x magnitude. Following structures are indicated on the image: SCT – syncytiotrophoblasts, MBC – maternal red blood cells, IS – intervillous space. Scale bar indicates 50 μm. **B** – Image at 20x magnitude. Three different villi are shown. Scale bar is set at 100 μm. **C** – Image at 10x magnitude. Following structures are denoted: SCT – syncytiotrophoblasts, CT – cytotrophoblasts, FC – fetal capillary. Scale bar is set at 200.